SARCOPENIA

Farnesol prevents aging-related muscle weakness in mice through enhanced farnesylation of Parkin-interacting substrate

Ju-Hyeon Bae[1,2]†, Areum Jo[3]†, Sung Chun Cho[4]†, Yun-Il Lee[4,5]†, Tae-In Kam[6,7]†, Chang-Lim You[1,2], Hyeon-Ju Jeong[1,2], Hyebeen Kim[1,2], Myong-Ho Jeong[1,2], Yideul Jeong[8], Young Wan Ha[9], Yu Seon Kim[4], Jiwoon Kim[4,10], Seung-Hwa Woo[4,10], Minseok S. Kim[10], Eui Seok Shin[9], Sang Ok Song[11], Hojin Kang[2,3], Rin Khang[2,3], Soojeong Park[2,3], Joobae Park[1], Valina L. Dawson[6,7,12,13,14,15,16], Ted M. Dawson[5,7,13,14,15,16]*, Sang Chul Park[4,17]*, Joo-Ho Shin[2,3,18]*, Jong-Sun Kang[1,2,8,18]*

Peroxisome proliferator–activated receptor-γ coactivator-1α (PGC-1α) is a master regulator of mitochondrial biogenesis. Reduced PGC-1α abundance is linked to skeletal muscle weakness in aging or pathological conditions, such as neurodegenerative diseases and diabetes; thus, elevating PGC-1α abundance might be a promising strategy to treat muscle aging. Here, we performed high-throughput screening and identified a natural compound, farnesol, as a potent inducer of PGC-1α. Farnesol administration enhanced oxidative muscle capacity and muscle strength, leading to metabolic rejuvenation in aged mice. Moreover, farnesol treatment accelerated the recovery of muscle injury associated with enhanced muscle stem cell function. The protein expression of Parkin-interacting substrate (PARIS/*Zfp746*), a transcriptional repressor of PGC-1α, was elevated in aged muscles, likely contributing to PGC-1α reduction. The beneficial effect of farnesol on aged muscle was mediated through enhanced PARIS farnesylation, thereby relieving PARIS-mediated PGC-1α suppression. Furthermore, short-term exercise increased PARIS farnesylation in the muscles of young and aged mice, whereas long-term exercise decreased PARIS expression in the muscles of aged mice, leading to the elevation of PGC-1α. Collectively, the current study demonstrated that the PARIS–PGC-1α pathway is linked to muscle aging and that farnesol treatment can restore muscle functionality in aged mice through increased farnesylation of PARIS.

INTRODUCTION

Aging is accompanied by progressive loss of skeletal muscle mass and strength, known as sarcopenia, leading to reduced functional capacity and an increased risk of developing chronic metabolic diseases (*1*–*4*). Among various treatments, exercise is the most effective approach for preventing and treating sarcopenia (*3*, *5*, *6*). Endurance exercise increases the proportion of oxidative muscle fibers rich in mitochondria with enhanced capacities for fatty acid oxidation and energy expenditure (*7*, *8*). Although the regulatory mechanism of exercise for prevention of sarcopenia is not yet fully understood, the induction of peroxisome proliferator–activated receptor-γ coactivator-1α (PGC-1α) seems to play a major role (*9*, *10*). PGC-1α is a transcriptional coactivator controlling genes involved in mitochondrial biogenesis, angiogenesis, and oxidative muscle metabolism (*11*, *12*). Mice lacking PGC-1α display decreased oxidative muscle metabolism and exercise capacity (*12*, *13*), whereas muscle-specific PGC-1α transgenic mice exhibit a protective effect against aging-related muscle wasting, leading to improvement of aging-associated whole-body health (*14*). Aging-related muscle loss leads to increased susceptibility to injury (*15*) and reduced regenerative capacity (*16*). Reduction of muscle regenerative capacity is associated with a decline in the number of satellite cells, muscle stem cells, and impaired responses to activation cues, leading to reduced proliferation or cellular senescence (*16*). The impairment in muscle regeneration is associated with elevated adipose and fibrotic tissues, a characteristic feature of sarcopenia (*17*, *18*). Muscle *PGC1A* overexpression protects muscles from damage by enhancing muscle regeneration mediated by mechanisms such as the modulation of immune responses favoring damage control, improved muscle satellite cell function, and suppression of fibrosis (*19*, *20*). Consistently, PGC-1α overexpression in muscle improves the maintenance of myogenic populations while suppressing

[1]Department of Molecular Cell Biology, Sungkyunkwan University School of Medicine, Suwon 440-746, South Korea. [2]Single Cell Network Research Center, Sungkyunkwan University School of Medicine, Suwon 440-746, South Korea. [3]Department of Pharmacology, Sungkyunkwan University School of Medicine, Suwon 440-746, South Korea. [4]Well Aging Research Center, Division of Biotechnology, DGIST, Daegu 42988, South Korea. [5]Department of Interdisciplinary Studies, DGIST, Daegu 42988, South Korea. [6]Neuroregeneration and Stem Cell Programs, Institute for Cell Engineering, Johns Hopkins University School of Medicine, Baltimore, MD 21205, USA. [7]Department of Neurology, Johns Hopkins University School of Medicine, Baltimore, MD 21205, USA. [8]Research Institute of Aging-related Diseases, AniMusCure Inc., Suwon 440-746, South Korea. [9]Well Aging Research Center, Samsung Advanced Institute of Technology, Samsung Electronics Co. Ltd., Suwon, Gyeonggi-do 446-712, South Korea. [10]Department of New Biology, DGIST, Daegu 42988, South Korea. [11]Standigm Inc., Seoul 06250, South Korea. [12]Department of Physiology, Johns Hopkins University School of Medicine, Baltimore, MD 21205, USA. [13]Solomon H. Snyder Department of Neuroscience, Johns Hopkins University School of Medicine, Baltimore, MD 21205, USA. [14]Department of Pharmacology and Molecular Sciences, Johns Hopkins University School of Medicine, Baltimore, MD 21205, USA. [15]Adrienne Helis Malvin Medical Research Foundation, New Orleans, LA 70130-2685, USA. [16]Diana Helis Henry Medical Research Foundation, New Orleans, LA 70130-2685, USA. [17]Future Life & Society Research Center, Chonnam National University, Gwangju 61469, South Korea. [18]Samsung Biomedical Research Institute, Samsung Medical Center, Seoul 06351, South Korea.
*Corresponding author. Email: kangj01@skku.edu (J.-S.K.); jshin24@skku.edu (J.-H. S.); scpark@snu.ac.kr (S.C.P.); tdawson@jhmi.edu (T.M.D.)
†These authors contributed equally to this work.

adipogenic populations, contributing to improved muscle regeneration (*21*). Thus, the up-regulation of PGC-1α in skeletal muscle may provide an avenue for the prevention and treatment of sarcopenia. Multiple studies have reported the protective effects of elevated PGC-1α against sarcopenia and aging-related metabolic diseases, such as type II diabetes and hepatic steatosis (*10*, *14*, *22*, *23*). The development of exercise mimetics that can replicate the effects of exercise on muscle strength via PGC-1α induction, like AICAR [5-aminoimidazole-4-carboxamide-1-β-D-ribofuranoside, adenosine monophosphate–activated protein kinase (AMPK) agonist] and metformin (anti-diabetes drug), has received interest for medication of muscle weakness caused by disease or aging (*24*–*27*). Previously, we identified PARIS (Parkin-interacting substrate, also known as ZNF746, harboring KRAB and C2H2-type zinc finger domains) as a repressor of PGC-1α in Parkinson's disease (PD) (*28*). PARIS is ubiquitinated by interaction with the E3 ligase Parkin and is subjected to a subsequent proteasomal degradation. PARIS has been shown to be increased in the absence of Parkin in patients with PD and in PD mouse models (*13*, *29*, *30*). Parkin has been linked to the maintenance of mitochondrial function and muscle integrity in flies and in patients with PD (*29*–*31*). Overexpression of *PARIS* in murine myoblasts elicited cellular senescence via oxidative stress–related forkhead box O1 (FoxO1) and p53 activation (*32*), suggesting a potential role for defective regeneration in aging muscle and sarcopenia. However, the physiological role of PARIS in the control of muscle function and metabolism is not yet defined.

Here, we identified a natural compound, farnesol, as a PGC-1α inducer in C2C12 myoblasts by high-throughput screening (HTS) and observed that farnesol administration prevented muscle weakness and metabolic misregulation in aged mice. In addition, farnesol treatment also enhanced muscle satellite cell proliferation and regenerative capacity. Short-term exercise and farnesol administration resulted in PGC-1α up-regulation by inhibiting PARIS through its farnesylation in skeletal muscles, whereas long-term exercise decreased PARIS expression, thereby enhancing PGC-1α. Thus, these data indicate that PARIS modulates muscle metabolism and functionality through regulation of PGC-1α. Together, these results suggest that farnesol might prevent muscle weakness related to aging or pathological conditions.

RESULTS

HTS for a PGC-1α inducer in skeletal muscle cells

HTS was used to identify compounds enhancing PGC-1α expression in stable C2C12 myoblasts expressing a luciferase reporter and destabilized green fluorescent protein (GFP) under control of the 1-kb human *PGC1A* promoter (Myo-PGC-1α). Myo-PGC-1α cells were treated with each of the 2552 compounds (the Spectrum Collection, MicroSource, 10 μM for 48 hours), and the HTS procedure was performed according to National Institutes of Health (NIH) guidelines (HTS Assay Guidance Criteria) (table S1, HTS assay protocol). The initial screen via luciferase assay identified eight compounds that increased the luciferase activity about 2.5-fold (Fig. 1A). These eight compounds were then independently re-screened in quadruplicate (Fig. 1B). To evaluate the robustness of HTS, standard parameters (plate-to-plate and day-to-day variations, signal-to-background ratio, coefficient of variation, and Z' factor) were assessed (fig. S1, A and B). Variations within and between plates and between days were minimal (fig. S1A). The Z' factor, an index of assay readiness for HTS, was within 0.5 to 1 range (fig. S1B).

Farnesol elevates PGC-1α and muscle oxidative metabolism in young mice

On the basis of its safety profile and potency, farnesol (CSU-1806), a natural 15-carbon organic compound found in *Alpinia conchigera*, *Lonicera japonica*, and other plants, was selected as an inducer of PGC-1α for this study. Farnesol satisfies the criteria for safe in vivo use according to the known rodent toxicity information [PubChem, mouse median lethal dose (LD_{50}): 8764 mg/kg]. In agreement with the screening data, C2C12 cells treated with 10 μM farnesol in the differentiation medium for 2 days exhibited a ~1.9-fold increase of PGC-1α proteins (Fig. 1C). Farnesol treatment also enhanced MyHC (myosin heavy chain)–positive myotube formation (fig. S1, C and D) relative to dimethyl sulfoxide (DMSO) treatment. Muscle-specific genes, including myoglobin (*Mb*), slow troponin T1 (*Tnnt1*), and mitochondrially encoded cytochrome C oxidase 1 (*Mt-Co1*), were up-regulated in farnesol-treated cells (fig. S1E). Farnesol increased PGC-1α protein in a dose-dependent manner up to 10 μM (fig. S1F). Unlike farnesol, geraniol and geranylgeraniol, which have similar structures to farnesol (*33*), had no effect on PGC-1α abundance (fig. S1G). Next, we asked whether the increase in mitochondria-related genes caused by farnesol is due to PGC-1α. To determine the PGC-1α–dependent effect of farnesol, we performed *Pgc-1α* knockdown by small interfering RNA (siRNA) in C2C12 myoblasts (fig. S1H) and the effect of farnesol on the expression of *Mt-Co1* and *Mb* was assessed (fig. S1I). *Pgc-1α* knockdown attenuated the effect of farnesol on the expression of *Mtco1* and *Mb*, suggesting that the effect of farnesol effect is dependent on PGC-1α. In addition, human muscle cells treated with 0.5 μM farnesol for 3 days differentiated faster (Fig. 1D) and expressed higher expression of *MYH2* and *MYH7* mRNA and PGC-1α protein compared with the DMSO-treated control (Fig. 1, E and F). These data suggested that the effect of farnesol was conserved between murine and human muscle cells.

To assess the effects of farnesol on muscle in vivo, 5-month-old C57BL/6J mice were fed with chow or farnesol diets (0.5% w/w) for 5 weeks. PGC-1α was substantially enhanced in tibialis anterior (TA) muscles of farnesol-fed mice (Fig. 1G). The increase in farnesol and farnesyl diphosphate (FPP), a substrate for farnesyl transferase (FTase), in the muscle was about 1.22 μg and 46.77 ng per gram of muscle weight in farnesol-fed mice, respectively (fig. S1, J and K). Farnesol treatment enhanced the proportion of MyHC-IIa–positive myofibers, giving a dark red appearance to muscles, whereas MyHC-IIb–positive myofibers were unchanged (Fig. 1I). Farnesol increased the cross-sectional area (CSA) of MyHC-IIa–positive myofibers in the extensor digitorum longus (EDL) (Fig. 1J). In quantitative reverse transcription polymerase chain reaction (qRT-PCR) analysis, oxidative myofiber–specific markers *MyHC-I* and *MyHC-IIa* were substantially elevated (threefold) in farnesol-TA compared with chow-TA (fig. S1L). In addition, farnesol administration enhanced *MyHC-IId/x* expression but had no effect on the expression of *MyHC-IIb*, the most glycolytic-type skeletal muscle marker. Among mitochondrial genes, *Mb* expression was increased about twofold and *Mt-Co1* was mildly decreased, whereas other mitochondrial genes such as *Sdh* and *Mt-Co2* were unchanged in farnesol-TA (fig. S1L). To further examine the farnesol effect on muscle

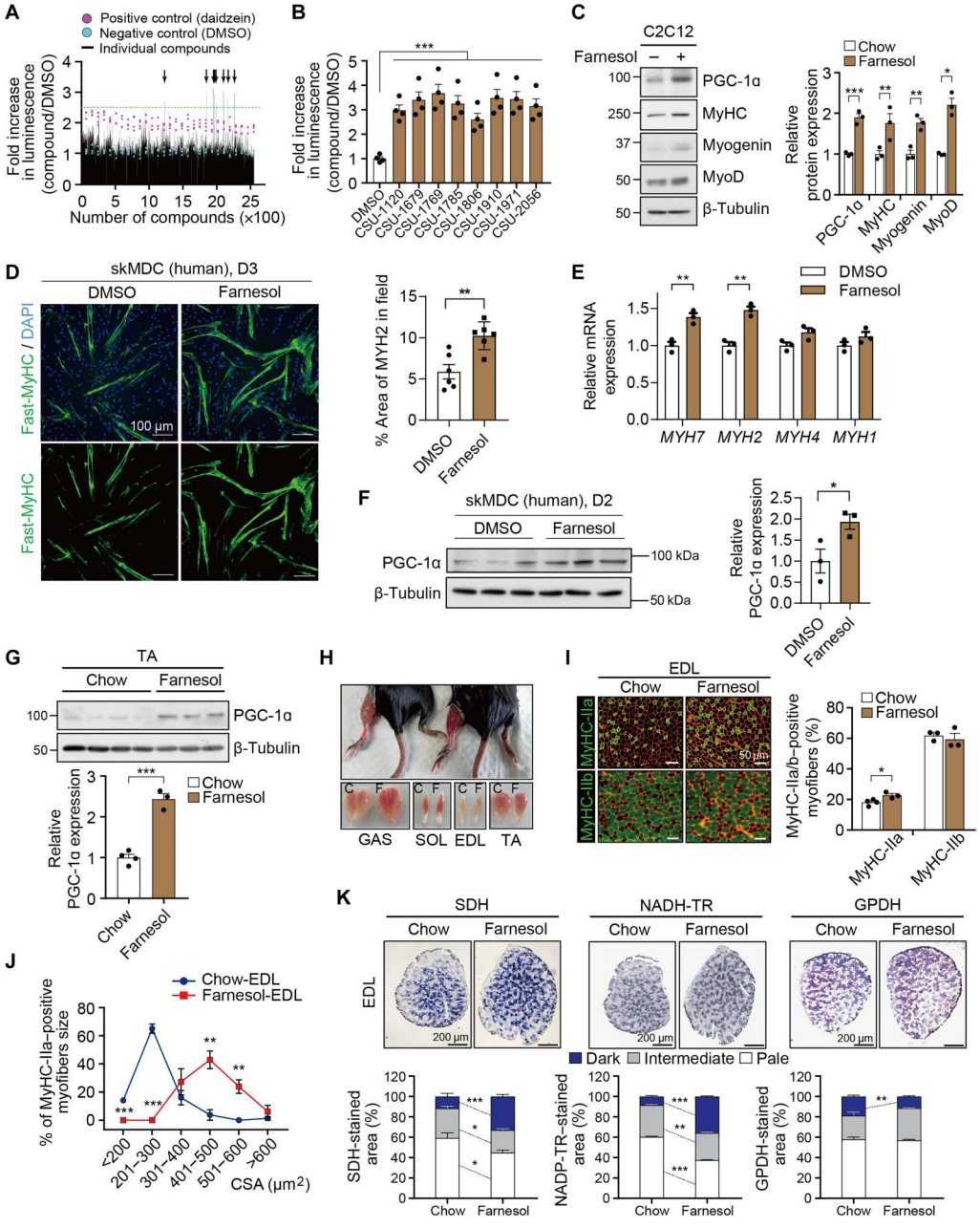

Fig. 1. Farnesol induces PGC-1α expression in skeletal muscles and switches toward oxidative metabolism. (**A**) Promoter activity of PGC-1α by luciferase assay for Myo-PGC-1α cells treated with each of 2552 compounds. The green dotted line indicates 2.5-fold activation. All readouts are displayed with color-coded shapes: blue circle (DMSO), red circle (daidzein), and black bar (experimental compounds). (**B**) Experiments performed in triplicate for the eight compounds showing >2.5-fold activation of PGC-1α. $n = 4$. (**C**) Immunoblot for PGC-1α and muscle marker proteins in C2C12 cells treated with DMSO or 10 μM farnesol for 2 days. Right: Quantification of the relative amounts of PGC-1α proteins. $n = 3$. (**D**) Immunostaining of fast-MyHC (green) expression in skMDC (human skeletal muscle–derived myoblast) treated with DMSO or 0.5 μM farnesol for 3 days. Scale bar, 100 μm. Right: Quantification of fast-MyHC area per field, n (field number) = 6. (**E**) qRT-PCR analysis for MyHCs (*MYH7*, *MYH2*, *MYH4*, and *MYH1*) in skMDC treated with DMSO or 0.5 μM farnesol for 3 days. 18*S* rRNA serves as an internal control. $n = 3$. (**F**) Immunoblot for PGC-1α in skMDC cells treated with DMSO or 0.5 μM farnesol for 2 days. Right: Quantification of the relative PGC-1α protein expression. $n = 3$. (**G**) Immunoblotting analysis for PGC-1α in TA muscles from 5-month-old mice fed with chow or farnesol diet for 5 weeks. Bottom: Quantitation of the immunoblots. $n = 4$, chow-fed; $n = 3$, farnesol-fed. (**H**) Representative photographs of isolated muscle groups from lower hindlimbs of 5-month-old mice fed with chow or farnesol diet for 5 weeks. C, chow-fed; F, farnesol-fed; GAS, gastrocnemius; SOL, soleus; EDL, extensor digitorum longus; TA, tibialis anterior. (**I**) MyHC-IIa or MyHC-IIb immunostaining of EDL muscles of 5-month-old mice fed with chow or farnesol diet for 5 weeks (left). Scale bar, 50 μm. Right: Quantification of MyHC-IIa/MyHC-IIb–positive myofibers in EDL muscles. Chow-MyHC-IIa, $n = 4$; chow-MyHC-IIb, $n = 3$; farnesol-MyHC-IIa, $n = 3$; and farnesol-MyHC-IIb, $n = 3$. (**J**) Quantification of the cross-sectional area (CSA) of MyHC-IIa–positive myofibers in EDL muscles of 5-month-old mice fed with chow or farnesol diet for 5 weeks. Values are expressed as a percentile. $n = 3$ per each group. (**K**) Histochemical staining for SDH, NADH-TR, and GPDH enzymatic activities in EDL muscles of 5-month-old mice fed with chow or farnesol diet for 5 weeks. Scale bar, 200 μm. The staining intensities are quantified as three different grades (dark, intermediate, and pale) and plotted as a percentile. $n = 3$. Data are expressed as mean ± SEM. Asterisk indicates statistical significance. $^*P < 0.05$, $^{**}P < 0.01$, and $^{***}P < 0.001$.

metabolic characteristics, cryosectioned muscles were examined for the activities of two mitochondrial enzymes, succinate dehydrogenase (SDH) and nicotinamide adenine dinucleotide–tetrazolium reductase (NADH-TR), and glycerol-3-phosphate dehydrogenase (GPDH) to monitor glycolytic activities. Farnesol treatment elevated the proportion of myofibers with strong staining intensities (dark) for SDH and NADH-TR, whereas it decreased dark stained myofibers and increased intermediately stained myofibers positive for GPDH compared with the control muscles (Fig. 1K). Together, these data suggested that farnesol induced the expression of PGC-1α in myoblasts and skeletal muscles, leading to an increase of oxidative muscle fibers.

Farnesol improves muscle strength and metabolic properties in aged mice

Next, we investigated the effect of farnesol treatment on the metabolism of aged mice (22-month-old) fed with chow or farnesol diet for 4 months. Farnesol treatment did not alter the parameters such as water/food intake, body mass, and lean mass of the aged mice (fig. S2, A to D). About 15% of gastrocnemius (GAS) muscle mass was reduced in aged mice compared with young mice (7-month-old, young GAS), and farnesol treatment did not alter this reduction (fig. S2E). Among PGC-1α isoforms, the hypertrophy-associated isoform PGC-1α-4 level (*34*) was unchanged, but the level of PGC-1α1 (identical to PGC-1α) and PGC-1α2/3 isoforms increased after farnesol treatment (fig. S2F). Farnesol treatment did not affect heart mass or heart fibrosis–related gene expression (fig. S2, G and H). In agreement with results obtained in young mice (Fig. 1, I and K), the proportions of MyHC-IIa myofibers and SDH- and NADH-TR–stained myofibers were increased in EDL of farnesol-fed 26-month-old mice compared with chow control (Fig. 2, A and B). Furthermore, farnesol treatment enhanced the expression of *MyHC-I*, *MyHC-IIa*, and *MyHC-IIb* as well as oxidative metabolic genes, *Mb*, *SDH*, and *Mt-Co1*, whereas *MyHC-IId/x* was down-regulated (fig. S2I).

To analyze the effect of farnesol on the muscle function of aged mice, farnesol was orally administrated to 26-month-old mice for 1 month, and muscle strength was measured in vivo and ex vivo. Farnesol-fed aged mice showed improvement in both twitch and tetanic force of soleus muscles compared with chow-fed aged mice (Fig. 2, C and D). In addition, farnesol-fed aged mice exhibited stronger grip strength (Fig. 2E) and enhanced energy expenditure than chow-fed aged mice (Fig. 2F and fig. S2J), whereas physical activity and rearing were comparable (fig. S2, K and L). These results suggested that farnesol treatment improves muscle contractile function in aged mice. This beneficial effect of farnesol was accompanied by improved metabolic properties, including improved glucose response (Fig. 2G), body fat mass ratio (Fig. 2H), fat accumulation in liver and white adipocytes (WAT) (Fig. 2I), and concentrations of cholesterols in blood (fig. S2, M and N). Blood triglyceride concentrations were not changed between farnesol- or chow-fed mice (fig. S2O). In particular, the decreased respiratory quotient after farnesol treatment might contribute to relatively high lipid oxidation and low-fat mass (fig. S2, P and Q).

Because PGC-1α has been shown to mediate exercise-induced angiogenesis in skeletal muscle (*35*), we analyzed the microvascular density by immunostaining of a vascular endothelial cell marker, CD31. Farnesol treatment increased the capillary density in muscles of young mice (fig. S3A) and aged mice (fig. S3B). Thus, angiogenesis might be contributing to the beneficial effect of farnesol in muscle function. Next, we examined the farnesol effect on fibrosis associated with muscle weakness and decreased regeneration capacities of aged muscles (*17*). As shown through picrosirius red staining, fibrosis was decreased in muscles from farnesol-fed aged mice compared with those from chow-fed mice (Fig. 2J). Consistently, fibrosis-related gene expression (*Tgfb1*, *Col1a1*, and *Timp2*) was also down-regulated in muscles from farnesol-fed mice compared with chow-fed mice (Fig. 2K). Collectively, farnesol treatment enhanced muscle function and oxidative metabolic muscle capacity, thereby contributing to enhanced energy expenditure and improved body metabolism.

Farnesol treatment enhances the regenerative capacity of satellite cells

Recent studies suggested that PGC-1α can enhance satellite cell activation and proliferation, thereby improving muscle regeneration (*19*, *20*, *36*). Therefore, we set out to determine the effect of farnesol on muscle regeneration using a cardiotoxin (CTX) injury model. Farnesol treatment augmented an increase in the average CSA of myofibers in TA muscles at 21 days after injury compared with vehicle groups (Fig. 3A). Fibrosis regions were also decreased in farnesol-treated groups compared with vehicle groups (Fig. 3A). Next, we have determined the effect of farnesol on proliferative capacity of satellite cells during muscle repair. TA muscles of vehicle- or farnesol-pretreated mice were subjected to CTX injury and injected with bromodeoxyuridine (BrdU) at 3 days after injury. After 24 hours, TA muscles were examined for BrdU incorporation. The vehicle-treated muscles had about 20% BrdU-positive cells, whereas the farnesol-treated muscles had about 30% BrdU-positive cells in the injured areas (Fig. 3B). In qRT-PCR analysis, cell cycle regulators [*Cyclin b1* (*Ccnb1*), *Ccnb2*, *Ccnd1*, *Ccne1*, *Ccnf*, *Minichromosome Maintenance Complex Component 3* (*Mcm3*), *Mcm7*, and *Aurora kinase B* (*AurkB*)] were elevated in farnesol-treated TA muscles (Fig. 3C). In addition, farnesol treatment substantially elevated *Myf5* expression, whereas the expression of *Pax7*, *MyoD*, and *Myogenin* (*Myog*) was not significantly changed compared to the vehicle treatment (Fig. 3C). To further examine the effect of farnesol on muscle stem cell activation upon injury, we performed fluorescence-activated cell sorting (FACS) analysis with TA muscles at 3 days after CTX injury. Farnesol treatment elevated the activated and proliferating population (Pax7, Myf5, or MyoD-positive cells), and Myog-positive cells were also increased by farnesol compared with vehicle (Fig. 3D). These results suggest that farnesol enhances muscle stem cell activation and proliferation in early repair. The number of Pax7-positive muscle stem cells was elevated by 1.39-fold in the farnesol-treated TA muscles at CTX 21 days after CTX injury compared with the vehicle-treated muscles (Fig. 3E). Moreover, farnesol-treated aged TA muscles had a small increase in Pax7-positive cells per 100 myofibers relative to the control aged muscles (Fig. 3F). In addition, we determined the percentile of myofiber size and myonuclei number of MyHC-IIa in the longitudinal sections of soleus from chow- or farnesol-fed young mice for 4 months. The average myonuclei number per MyHC-IIa myofiber significantly increased by 1.5- to 1.7-fold (1000 to 3000 μm^2, $P = 0.001$; 3001 to 6000 μm^2, $P = 0.002$; >6000 μm^2, $P = 0.013$) in farnesol-fed soleus than in chow-control soleus (fig. S4, A to C). Together, these data suggested that farnesol improved muscle regeneration capacity by enhancing muscle stem cell proliferation and maintenance.

Farnesol reverses age-related mitochondrial alterations in aged mice

Muscle aging is associated with alterations in mitochondrial contents, function, and gene expression (*37*, *38*). To determine the effect of farnesol on mitochondria, we orally administrated vehicle or farnesol to 26-month-old male mice for 1 month, and muscles were subjected to analysis for mitochondrial DNA (mtDNA) content and total oxidative phosphorylation (OXPHOS) proteins. The results revealed that the mtDNA content was increased about 1.6-fold ($P = 0.038$), and adenosine triphosphate (ATP) synthase F1 subunit α (ATP5A), ubiquinol-

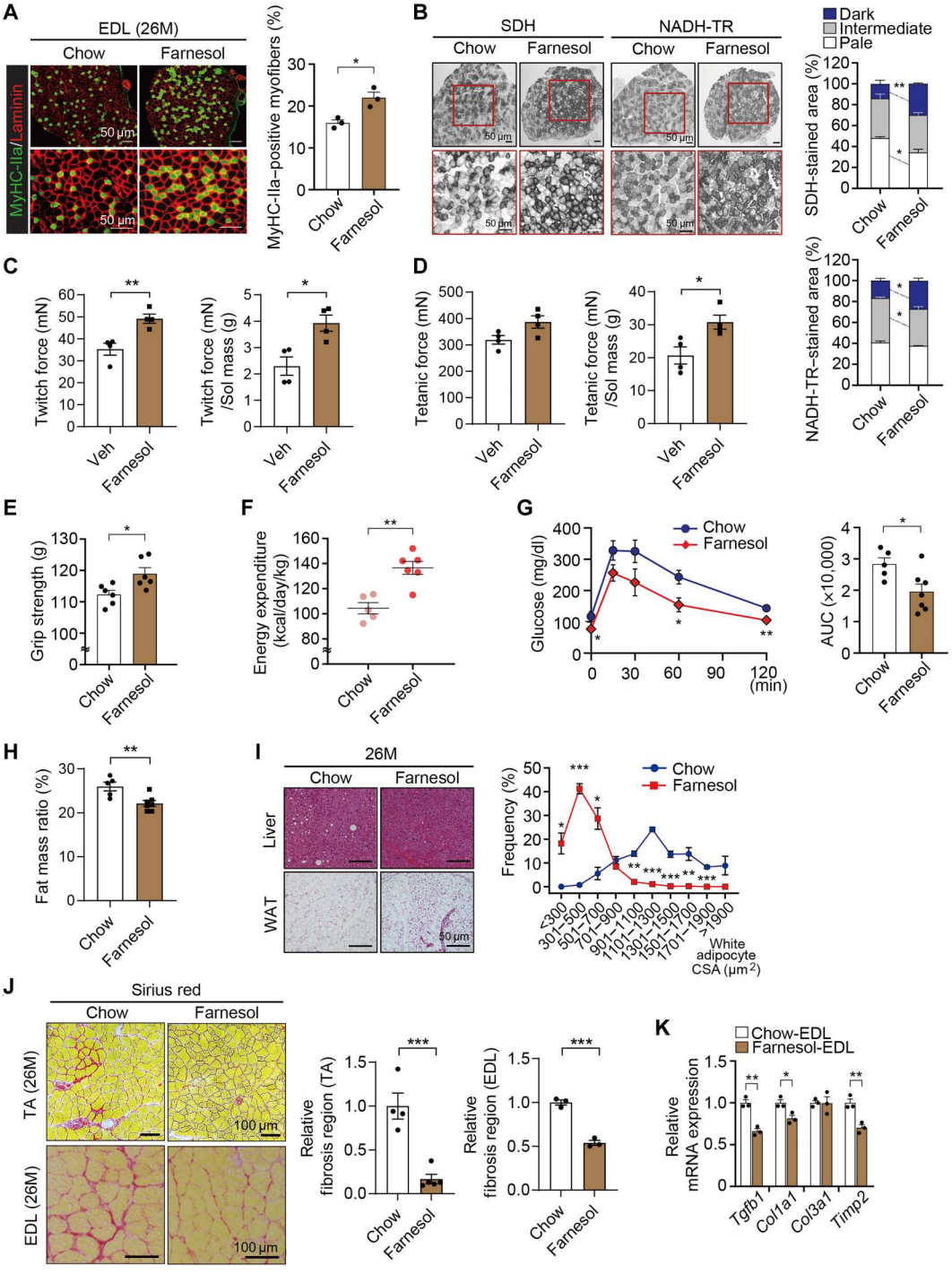

Fig. 2. Farnesol enhances oxidative muscle capacities and strength in aged mice. (**A**) Immunostaining of MyHC-IIa (green) and laminin (red) in the EDL muscles of 26-month-old mice ± farnesol diet. Scale bar, 50 μm. Right: Quantification of MyHC-IIa–positive myofibers, plotted as a percentile of MyHC-IIa–positive myofibers. $n = 3$. (**B**) Representative histochemical staining of SDH and NADH-TR enzymatic activities in the EDL muscles of 26-month-old mice fed with chow or farnesol diet for 4 months. Scale bar, 50 μm. The staining intensities are quantified as three different grades (dark, intermediate, and pale) and plotted as a percentile. $n = 3$. (**C**) Twitch force (mN) and normalized twitch force [mN/g (muscle mass)] of soleus (Sol) muscles from orally administrated vehicle (Veh)– or farnesol-treated 26-month-old mice. $n = 4$. (**D**) Tetanic force (mN) and normalized tetanic force [force (mN)/muscle mass (g)] of (C) mice muscles. $n = 4$. (**E**) Grip strength depicted as the gram (g) that animals in each group pulled. $n = 6$. (**F**) Energy expenditure measured with 26-month-old mice ± farnesol diet (4 months) over 1 day using metabolic cages. Chow, $n = 5$; farnesol, $n = 6$. (**G**) Glucose tolerance test and quantification [area under the curve (AUC), right] of glucose clearance from 26-month-old chow- and farnesol-fed mice. Chow, $n = 5$; farnesol, $n = 7$. (**H**) Fat mass ratio for chow- or farnesol-fed aged mice. Chow, $n = 5$; farnesol, $n = 7$. (**I**) Hematoxylin and eosin (H&E) staining of liver and white adipose tissue (WAT) from 26-month-old mice ± farnesol diet (4 months). Scale bar, 50 μm. Quantification of CSA of white adipose cells plotted as a percentile. $n = 3$. (**J**) Picrosirius red staining of TA (top) and EDL (bottom) muscles from 26-month-old mice ± farnesol diet (4 months). Scale bar, 100 μm. Quantification of fibrotic tissue (red) area as relative value. TA: chow, $n = 4$; farnesol, $n = 5$; EDL: chow, $n = 3$; farnesol, $n = 3$. Data are expressed as mean ± SEM. (**K**) qRT-PCR analysis for fibrosis-related genes in the EDL muscles of aged mice ± farnesol diet. An unpaired two-tailed Student's t test (A to K) was used for statistical analysis. Differences were considered significant when $^*P < 0.05$, $^{**}P < 0.01$, and $^{***}P < 0.001$.

cytochrome c reductase core protein 2 (UQCRC2), MT-CO1, and SDH complex, subunit B, iron sulfur (Ip) (SDHB) proteins were significantly elevated in farnesol-treated TA muscles compared with vehicle-treated muscles (ATP5A, 2.2-fold, $P = 0.039$; UQCRC2, 2.4-fold, $P = 0.011$; SDHB, 2.1-fold, $P = 0.031$). To examine the effect of farnesol on mitochondrial function, C2C12 myoblasts were treated with vehicle or farnesol, and oxygen consumption rates (OCRs) were assessed (fig. S5A). The maximal OCR was not significantly elevated by farnesol treatment. However, farnesol treatment did increase mtDNA content about 1.5-fold in C2C12 myoblasts (fig. S5B) and OXPHOS proteins, specifically NADH:

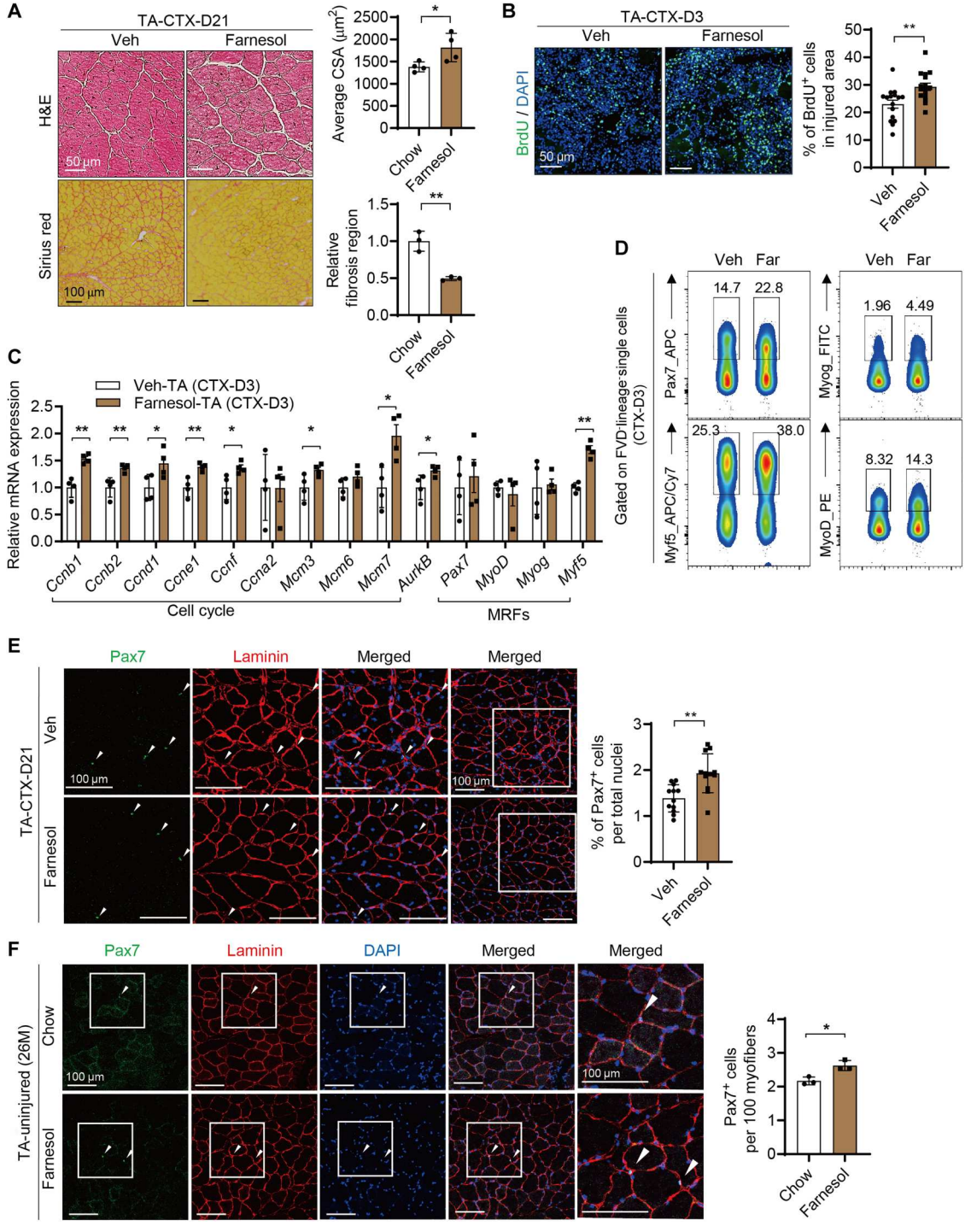

Fig. 3. Farnesol enhances muscle regeneration capacity. (**A**) Top: H&E staining for histological analysis of TA muscles from vehicle- or farnesol-treated mice at CTX-D21. Scale bar, 50 μm. Quantification of average CSA of TA muscles from vehicle- or farnesol-treated mice at CTX-D21. *n* = 4. Bottom: Sirius red staining of TA muscles from vehicle- or farnesol-treated mice at CTX-D21. Scale bar, 100 μm. Quantification of fibrosis regions of TA muscles from vehicle- or farnesol-treated mice at CTX-D21. *n* = 3. (**B**) Immunostaining for BrdU (green) from vehicle- or farnesol-treated TA at CTX-D3. Percentage of BrdU-positive cells in fields. *n* = 4. (**C**) qRT-PCR analysis for cell cycle regulators and myogenic regulatory factors (MRFs) in TA muscles at CTX-D3. 18*S* rRNA served as an internal control. (**D**) FACS analysis for muscle stem cell populations in TA muscles from vehicle- or farnesol-treated mice at CTX-D3. Cells were pregated by fixable viability dyes (FVD) and lineage markers [CD31, CD45, CD106, and Ly6A/E; phycoerythrin (PE)/Cy7] for analysis of Pax7 [allophycocyanin (APC)], Myf5 (APC/Cy7), Myog [fluorescein isothiocyanate (FITC)], and MyoD (PE). Percentage values of positive cells are indicated in each graph. (**E**) Immunostaining for Pax7 (green) and laminin (red) of TA muscles from vehicle- or farnesol-treated mice at CTX-D21. Quantification of Pax7-positive cells. Fifteen fields per three sections from each muscle. *n* = 4. (**F**) Immunostaining for Pax7 (green) and laminin (red) of TA muscles from chow- or farnesol-fed mice at 26 months old. Quantification of Pax7-positive cells. Fifteen fields per three sections from each sample. *n* = 3. Data are expressed as mean ± SD.

ubiquinone oxidoreductase subunit B8 (NDUFB8) protein (fig. S5C).

To further investigate the effect of farnesol in aged muscles, RNA-sequencing analysis was performed on GAS muscles from vehicle- or farnesol-fed 26-month-old mice. The gene ontology (GO) analysis of the differentially expressed genes (DEGs) indicated that mitochondrial genes were listed second among cellular compartment–related genes (Fig. 4C). Most mitochondrial genes in farnesol-treated muscles showed increased expression compared with those in vehicle-treated group (Fig. 4D). To further analyze, the altered expression of mitochondrial genes in the farnesol-treated muscles was compared with the altered mitochondrial genes in 28-month-old muscles versus 8-month-old muscles from the Sarcoatlas gene expression database (https://sarcoatlas.scicore.unibas.ch/) (*39*). Farnesol treatment in aged muscles reversed the expression of mitochondrial genes altered in aged muscles compared with young muscles (Fig. 4E). Gene expressions of other GO terms such as OXPHOS, skeletal muscle tissue development, fatty acid β oxidation, and skeletal muscle contraction were also substantially altered in farnesol-treated muscles compared with vehicle-treated aged muscles (Far/Veh) (fig. S6). Further GO analysis of the mitochondrial genes from Fig. 4D revealed that the genes related to mitochondrial organization and oxidative stress response appeared to be most affected by farnesol treatment (Fig. 4F). These genes were mostly up-regulated in the farnesol-treated muscles, whereas they were mostly down-regulated in the 28M/8M dataset from Sarcoatlas (Fig. 4, G and H). In addition, transforming growth factor–β (TGF-β) signaling gene expression showed a reversed pattern in Far/Veh compared with 28M/8M from Sarcoatlas (fig. S6). These data are in line with the decreased fibrosis in farnesol-fed aged mice (Fig. 2, J and K). Together, these data suggested that farnesol administration improved mitochondrial biogenesis capacity and reversed age-related mitochondrial gene expression patterns.

Farnesol blunts PARIS-mediated changes in skeletal muscles

Exercise induces PGC-1α by activating signaling pathways such as AMPK and p38 mitogen-activated protein kinase (p38) (*9*, *27*, *40*). To determine the involvement of AMPK and p38 in farnesol-mediated PGC-1α induction, control- or farnesol-treated C2C12 cells were analyzed by immunoblotting (Fig. 5A). The active phosphorylated forms of AMPK (p-AMPK) and p38 (p-p38) were unchanged by farnesol treatment. In addition, farnesol treatment did not alter the phosphorylated forms of mechanistic target of rapamycin kinase (mTOR) and its downstream targets, eukaryotic translation initiation factor 4E binding protein 1 (4EBP-1) and ribosomal protein S6 (S6) (fig. S7). Previously, we identified the accumulation of PARIS in the loss of Parkin, suppressing PGC-1α transcription in PD (*28*). To gain insights into the PARIS/PGC-1α relationship in human muscles, we have analyzed public open datasets from human aged and post-exercise muscles for the *PGC-1α* and *PARIS* correlation [Gene Expression Omnibus (GEO) accession: GSE111017 and GSE117525]. In two datasets, *PGC-1α* and *PARIS* exhibited a negative correlation, consistent with our observations in this study (fig. S8, A and B) (*38*, *41*). We then determined the expression of Parkin, PARIS, and PGC-1α in muscles from 24-month-old mice (24M). PARIS was elevated, whereas Parkin and PGC-1α were decreased, in TA of 24M as compared with young mice (4M) (Fig. 5B). PARIS expression was also assessed in diverse muscle fibers of young mice. PARIS was expressed at lower expression in soleus muscles, which are known to contain predominantly oxidative fibers expressing high PGC-1α expression (*12*), relative to other hindlimb muscles, which contain various proportions of oxidative and glycolytic fibers (Fig. 5C). Although farnesol treatment enhanced oxidative metabolism in aged mice (Fig. 2), PARIS expression in TA muscles was unchanged by 5-week farnesol treatment in aged mice (Fig. 5D), indicating that farnesol does not modulate PARIS protein expression.

To examine the effect of PARIS on oxidative metabolism in muscle cells, control or pCMV-PARIS–expressing C2C12 cells were induced to differentiate for 3 days, followed by MyHC immunostaining. *PARIS* overexpression in C2C12 cells caused the reduction of PGC-1α and the formation of MyHC-positive myotubes as compared with control, which was substantially reversed by farnesol treatment (Fig. 5, E and F, and fig. S9A). In addition, *PARIS* overexpression significantly decreased the expression of genes involved in oxidative metabolism as assessed by qRT-PCR (fig. S9B).

Next, lentiviral-GFP or lentiviral-PARIS/GFP was injected into TA muscles of 22-month-old mice by a stereotactic procedure. Seven days after virus injection, muscles were harvested and examined by histological staining and qRT-PCR. To evaluate the efficiency of lentiviral transduction, cryosectioned muscles were subjected to immunostaining for GFP expression. GFP expression was detected in a large portion of myofibers, and *PARIS* mRNA expression was strongly induced in lentiviral-PARIS/GFP–injected muscles (fig. S9, C and D). PARIS-overexpressing muscles displayed a reduction in myofibers with dark SDH enzymatic staining, which correlated with decreased expression of *Pparcg1a* and oxidative fiber genes as compared with control muscles (fig. S9, D to F). Conversely, fibrosis-related genes were substantially increased in PARIS-overexpressing TA muscles (fig. S9E).

To examine the effects of farnesol on PARIS-mediated metabolic changes, 22-month-old mice were fed with chow or farnesol diet (0.5% w/w) starting at 1 week before injection with either lentiviral-GFP or lentiviral-PARIS/GFP viruses into skeletal muscles. Mice were fed with chow or farnesol diet for an additional 7 days after lentiviral injection and were subjected to SDH activity staining. The decrease of SDH activity by PARIS overexpression was restored almost to the control expression by farnesol administration (fig. S9F). Next, we examined whether the metabolic changes induced by PARIS and farnesol were accompanied by alteration in mitochondrial contents. The 22-month-old mice were fed with chow or farnesol diet for 1 week before injection with adeno-associated virus (AAV)–GFP or AAV-PARIS viruses into TA muscles and fed for additional 3 weeks, followed by analysis for mtDNA and total OXPHOS protein. Farnesol-treated AAV-GFP–infected muscles exhibited an increase in mtDNA content, whereas *PARIS*-transduced muscles had decreased mtDNA content. However, farnesol failed to elevate mtDNA in AAV-PARIS–transduced muscles (Fig. 5G). Farnesol treatment in AAV-GFP muscles increased total OXPHOS protein, whereas AAV-PARIS transduction significantly reduced NDUFB8, SDHB, MT-CO1, and UQCRC2 proteins (Fig. 5H). Furthermore, AAV-PARIS transduction abrogated the induction of total OXPHOS proteins by farnesol. These data collectively suggested that the accumulation of PARIS in aged muscle led to decreased oxidative metabolism that could be restored by farnesol treatment.

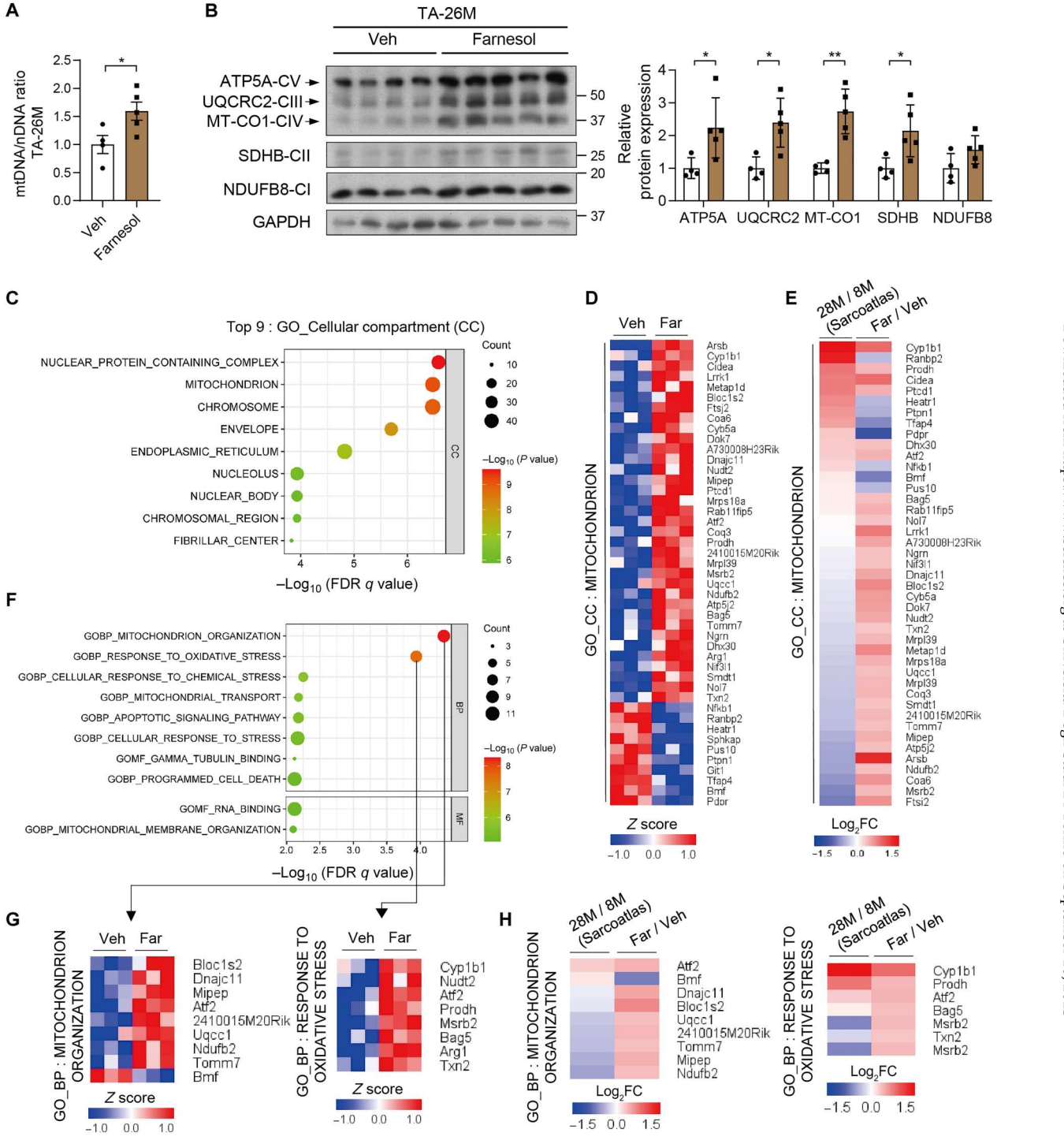

Fig. 4. Mitochondrial alteration profile in skeletal muscle of aged mice after farnesol treatment. Mice (26 months old) were orally administrated with vehicle or farnesol (350 mg/kg) for 30 days. (**A**) Relative mitochondrial DNA (mtDNA; *Mt-Co2*) versus nuclear DNA (nDNA; β-*actin*) in GAS muscles. $n = 4$, vehicle; $n = 5$, farnesol. (**B**) Immunoblotting analysis for total OXPHOS in TA muscles from vehicle- or farnesol-treated mice. Right: Quantitation of the immunoblots. $n = 4$, vehicle; $n = 5$, farnesol. (**C** to **H**) Transcriptome analysis for GAS muscles from vehicle- or farnesol-treated mice. $n = 3$, vehicle; $n = 3$, farnesol. Global DEGs are selected by cutoff parameters [fold change (FC) < 1.25 and $P < 0.05$]. (C) Bubble plot representing top nine significant GO terms for category of cellular compartment (CC) were selected on the basis of their nominal P value ($-\log_{10}$) and false discovery rate (FDR) q value ($-\log_{10}$). (D) Heatmap showing up- or down-regulated genes among GO terms of mitochondrion. (E) Left heatmap displaying $\log_2$ fold change of mitochondrion genes from significantly expressed genes (FDR $q < 0.05$) in GAS muscles from 28-month-old ($n = 8$) or 8-month-old ($n = 9$) mice. Transcriptome results were obtained from Sarcoatlas. Right heatmap showing $\log_2$ fold change of genes from Far/Veh. (F) Key GO terms for category of biological process (BP) or molecular function (MF) among mitochondrion gene sets at (D). (G) Heatmap showing up- or down-regulated gene lists at (D) among represented top GO terms. (H) Heatmap showing $\log_2$ FC of genes from 28M/8M or Far/Veh. Data are expressed as mean ± SD.

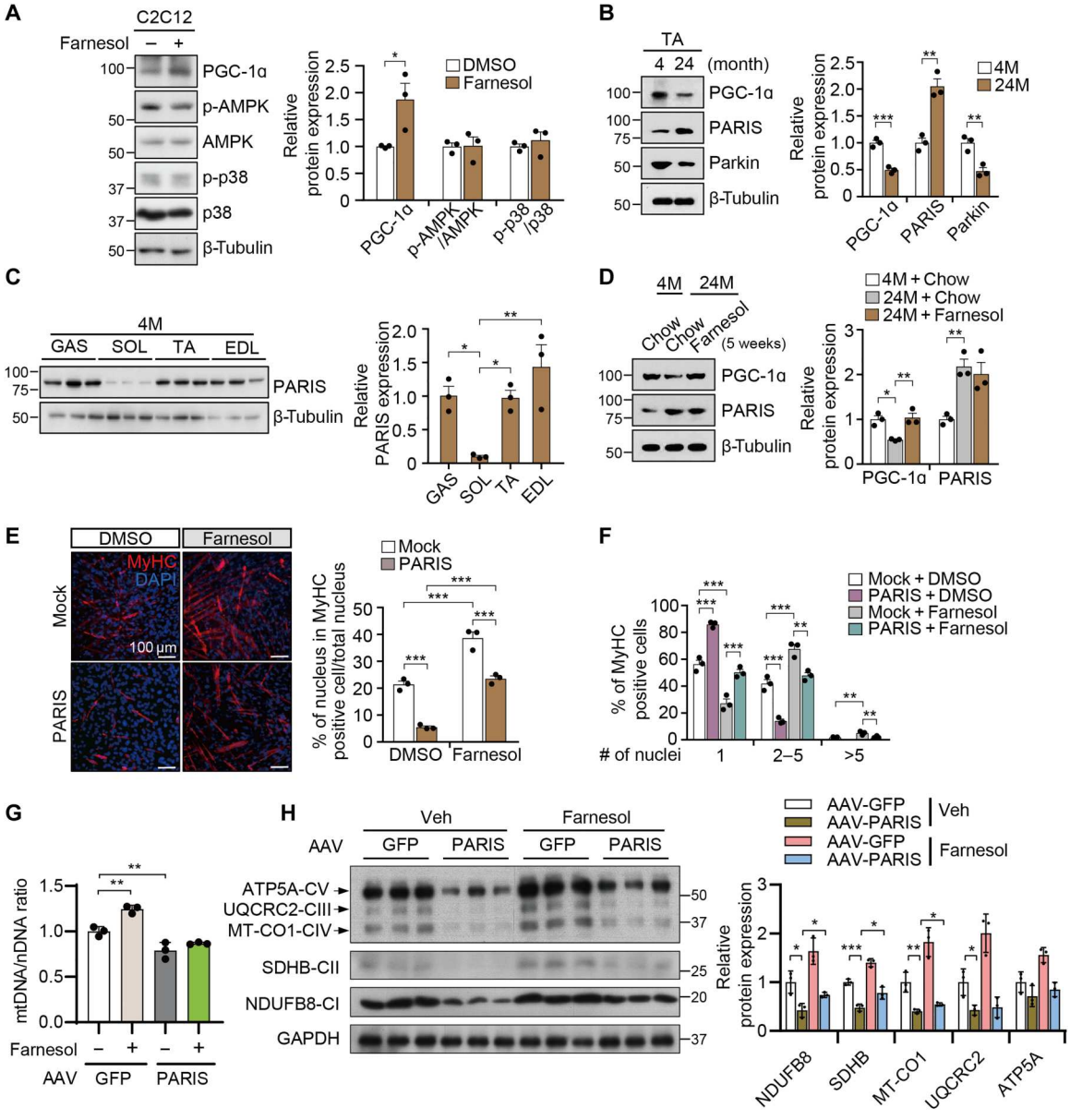

Fig. 5. Farnesol blunts PARIS-mediated changes in mouse skeletal muscle. (**A**) Representative immunoblot images of PGC-1α, p-AMPK, p-p38, and total AMPK, p38 in C2C12 cells treated with DMSO or 10 μM farnesol for 24 hours. Right: Quantitation of the immunoblots. $n = 3$. (**B**) Immunoblot analysis of PGC-1α, PARIS, and Parkin in TA muscles from young (4-month-old) and aged (24-month-old) mice. Quantification of PGC-1α, PARIS, and Parkin proteins. $n = 3$. (**C**) Immunoblot analysis of PARIS in murine hindlimb muscles; GAS, SOL, TA, and EDL, $n = 3$. Right: Quantitation of the immunoblots. (**D**) Immunoblot analysis of PGC-1α and PARIS expression in TA muscles of young mice, aged mice, or farnesol-fed aged mice. Farnesol diet was given for 5 weeks. Right: Quantitation of the immunoblots. $n = 3$. (**E**) Immunostaining of MyHC expression in C2C12 cells transfected with pCMV control (Mock) or pCMV-PARIS expression vector (PARIS) along with DMSO or farnesol treatment. Scale bar, 100 μm. Right: Quantification of myotube formation. C2C12 cells were scored as MyHC positive or negative. $n = 3$. (**F**) MyHC-positive cells were further scored by the number of nuclei (1, 2 to 5, or >5). $n = 3$. (**G**) Relative mtDNA (*Mt-Co2*) versus nDNA (*β-actin*) in TA muscles. $n = 3$. (**H**) Immunoblotting analysis for total OXPHOS in TA muscles from vehicle- or farnesol-treated mice. Right: Quantitation of the immunoblots. $n = 3$. Data are expressed as mean ± SEM.

Farnesol enhances PARIS farnesylation, regulating PGC-1α in skeletal muscles

The role of PARIS in farnesol effects was examined with C2C12 cells transfected with *siPARIS*. The knockdown of *PARIS* led to a twofold increase in PGC-1α in C2C12 as shown in SH-SY5Y cells (fig. S9G) (*28*, *29*). Farnesol failed to increase PGC-1α expression in the absence of PARIS, suggesting that PARIS is required for PGC-1α induction by farnesol (fig. S9G).

Farnesol can activate both peroxisome proliferator–activated receptor α (PPARα) and PPARγ in vitro (*42*). We next investigated whether farnesol regulates PGC-1α via PPARα and PPARγ. Farnesol was ineffective on PPARα and PPARγ protein and mRNA expression (fig. S9, G and H), as well as mRNA expression of PPAR

common target genes, including acyl-coenzyme A (CoA) oxidase 1 (*Acox1*), medium-chain specific acyl-CoA dehydrogenase (*Acadm*), long-chain specific acyl-CoA dehydrogenase (*Acadl*), and carnitine O-palmitoyltransferase 1 (*Cpt1a*) (fig. S9H). In addition, there was no luciferase promoter activation of PPAR-responsive element (PPRE) by farnesol treatment in C2C12 cells transfected with either siPARIS or Flag-PARIS (fig. S9I). Together, these findings suggested that the effects of farnesol in C2C12 cells were independent of PPARα/γ activation.

The fact that farnesol is a key substrate for protein farnesylation led us to investigate whether farnesol regulates PARIS through farnesylation. C2C12 cells were treated with DMSO or farnesol for 48 hours, and the endogenous PARIS immunoprecipitate was subjected to immunoblotting using anti-farnesyl antibodies. Farnesol treatment increased PGC-1α and the farnesylated PARIS proteins without altering total PARIS abundance (fig. S10A). To determine whether farnesol treatment increases PARIS farnesylation in vivo, PARIS was immunoprecipitated from TA muscles of mice fed with chow or farnesol diet for 7 days. PARIS was endogenously farnesylated in chow-TA muscles, and farnesol diet further enhanced the abundance of farnesylated PARIS, which was accompanied by the time-dependent up-regulation of PGC-1α (Fig. 6A). Next, we investigated whether farnesylation altered the localization of PARIS in myoblasts by PARIS immunostaining in response to DMSO or farnesol treatment, showing that there was no significant alteration in PARIS nuclear localization in response to farnesol (fig. S10B). Farnesylation is a posttranslational lipidation of proteins with isoprenoids by which FTase uses farnesol's intermediates, FPP, to modify cysteine residues at C termini with a CaaX motif (C is cysteine, a is an aliphatic amino acid, and X is a preferentially methionine or serine) (*43*). We found a putative CaaX motif near the C terminus of PARIS at ^{631}CGLS^{634}. To assess whether the effect of farnesol on PGC-1α is mediated by PARIS farnesylation, we transfected C2C12 cells with Flag-PARIS wild-type (WT) or Flag-PARIS C631S, which has substituted the cysteine at amino acid 631 with serine (C631S) to remove the putative farnesylation site in human PARIS, and examined the effect of farnesol on PGC-1α and PARIS farnesylation. Farnesol treatment induced a robust increase in farnesylation in PARIS WT, which was abrogated in PARIS C631S. This effect on farnesylation of PARIS WT correlated with PGC-1α up-regulation, whereas farnesol had no significant effect on PGC-1α expression in cells expressing PARIS C631S (Fig. 6B and fig. S10C). C2C12 cells transfected with Flag-PARIS WT or Flag-PARIS C631S were differentiated for 2 days and were subjected to MyHC immunostaining. The results revealed that farnesol alleviated the inhibitory effect of Flag-PARIS WT on myotube formation, but it had no effect on cells expressing Flag-PARIS C631S (Fig. 6C and fig. S10D).

To evaluate the effect of PARIS farnesylation in muscle, mice were fed with chow or farnesol diet for 7 days before injection with AAV-GFP, AAV-PARIS WT, or AAV-PARIS C631S viruses to TA muscles. After injection, mice were fed for an additional 14 days with chow or farnesol diet, followed by histochemical analysis. TA muscles transduced with AAV-PARIS WT and AAV-PARIS C631S showed a reduction of myofibers with dark SDH enzymatic staining compared with the control AAV-GFP muscles (Fig. 6D). Farnesol alleviated the reduction of oxidative muscle metabolism caused by AAV-PARIS WT but not by AAV-PARIS C631S (Fig. 6D). Together, these data suggested that the effect of farnesol on oxidative metabolism was mediated through PARIS farnesylation in muscle.

Next, we used PARIS C638S knock-in (C638S KI) mice harboring genomic substitution of murine cystein^{638}, which is conserved position to the cysteine^{631} at CGLS motif of human PARIS, to serine by the CRISPR-Cas9 system (fig. S10E) to understand the physiological role of PARIS farnesylation in vivo. Immunoblot analysis revealed that the farnesylation signal of PARIS was not detected in the GAS of C638S KI mice as compared to that of WT mice, revealing that the murine CGLS motif is an endogenous target for farnesylation in skeletal muscle (Fig. 6E). The loss of PARIS farnesylation was accompanied by PGC-1α reduction (Fig. 6E), supporting the notion that PARIS farnesylation is important for PGC-1α induction in vivo. Furthermore, farnesol enhanced the percentage of MyHC-IIa myofibers in WT mice but not in PARIS C638S KI mice (Fig. 6F).

PARIS is an exercise-related factor in mouse skeletal muscle

Given that PGC-1α is a major regulator mediating exercise effect, we examined whether PARIS farnesylation was involved in the exercise effect. Four- or 22-month-old mice were subjected to a mild-endurance exercise for 5 days (short term) with a treadmill. Immunoblot analysis revealed that short-term exercise increased the abundance of PGC-1α and of PARIS farnesylation with no change of total PARIS in both exercised young and old GAS as compared to those of non-exercised GAS (Fig. 7A). The relative abundance of farnesylated PARIS normalized by total PARIS was comparable between young and old GAS, although the total abundance of PARIS in old GAS was increased. However long-term exercise (5 weeks) resulted in the up-regulation of PGC-1α and PARIS down-regulation, but not PARIS farnesylation in old GAS as compared with non-exercised GAS (Fig. 7B), suggesting that exercise-mediated molecular alterations of PARIS in muscles were exercise duration dependent. To understand whether PGC-1α induction by AICAR is mediated by PARIS, a known exercise mimetic involved in PARIS farnesylation, C2C12 cells were exposed to AICAR, and immunoblot analysis was performed. AICAR treatment enhanced the expression of AMPK activation as previously reported (*24*) (fig. S11), whereas there was no change of PARIS farnesylation, suggesting that PGC-1α induction by AICAR does not involve PARIS farnesylation (fig. S11).

Farnesol restores PGC-1α abundance in muscles of high-fat diet–fed mice

Because farnesol administration increases PGC-1α and regulates exercise-mediated molecular alterations, we examined the effects of farnesol on high-fat diet (HFD)–induced muscle weakness associated with decreased PGC-1α expression and mitochondrial abnormalities (*44*). After 12 weeks of HFD, mice exhibited several metabolic alterations, including body weight gain, enhanced fat mass, hepatic fat accumulation, larger CSA of adipocytes, and glucose intolerance, as compared with standard diet (STD)–fed mice without any significant alteration of food intake (Fig. 7, C and D, and fig. S12, A to D). These effects were ameliorated by co-administration of farnesol or metformin, which was used as an anti-obesity drug (positive control) (Fig. 7, C and D, and fig. S12, B to D). Despite improved metabolism, there were no differences in muscle weights among the groups (fig. S12E). The GAS muscles of 6-month-old mice fed with HFD along with farnesol or metformin

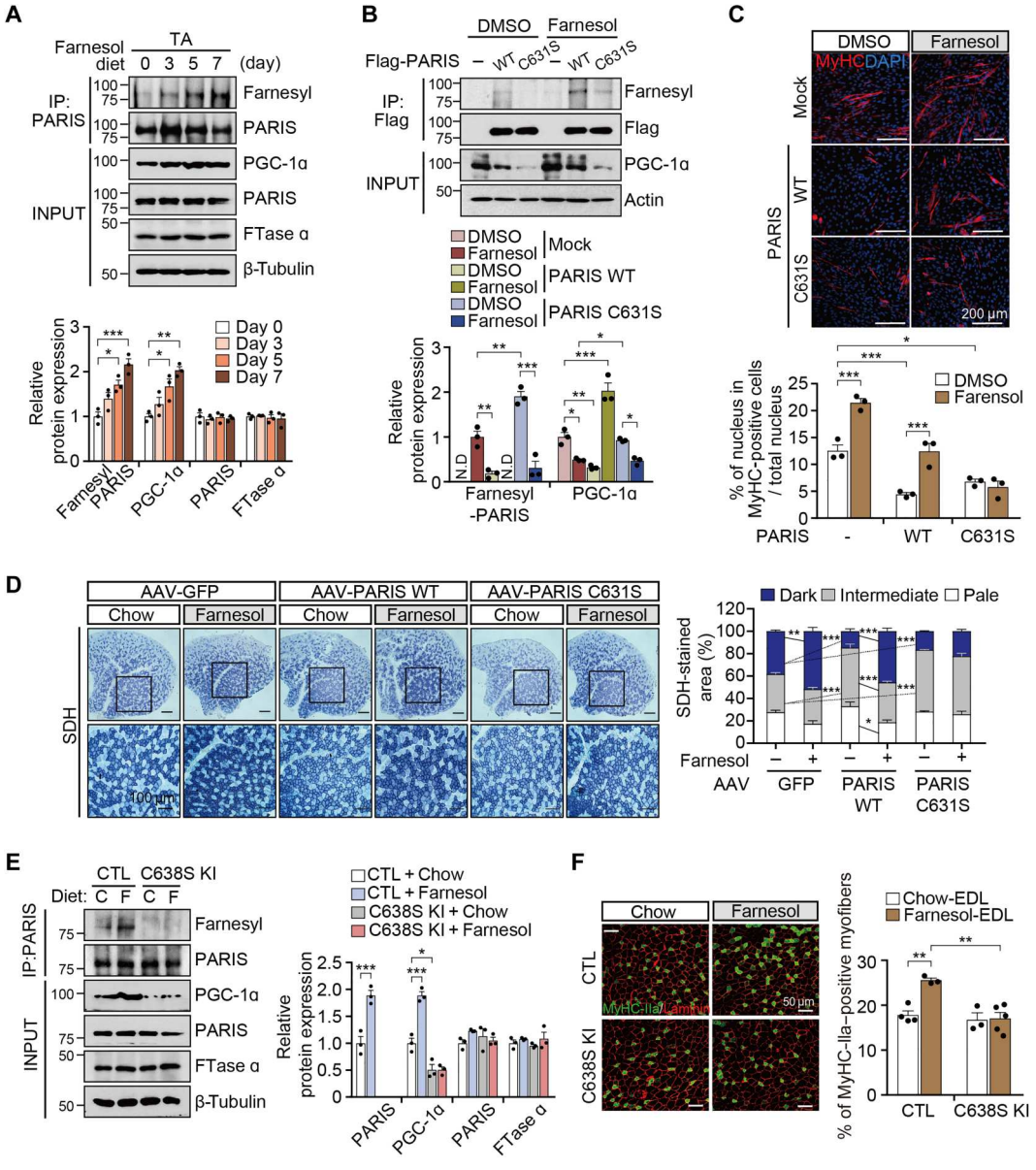

Fig. 6. Farnesol induces PGC-1α and oxidative metabolism through PARIS farnesylation. (**A**) Immunoblot analysis of PARIS farnesylation in the TA muscles of mice fed with farnesol diet for 0, 3, 5, or 7 days. Bottom: Quantification of PGC-1α and farnesylated PARIS. $n = 3$. (**B**) Representative immunoblot images of PARIS farnesylation and PGC-1α in C2C12 cells transfected with PARIS WT or C631S mutant ± farnesol (10 μM, 48 hours). Bottom: Quantification PARIS farnesylation. $n = 3$. (**C**) Immunostaining of MyHC expression in C2C12 cells transfected with PARIS WT or C631S ± farnesol at day 3 of differentiation. Scale bar, 200 μm. Bottom: Quantification of myotube formation. $n = 3$. (**D**) Histological staining for SDH activities in TA muscles injected with control AAV-GFP, AAV-PARIS WT, or AAV-PARIS C631S viruses and treated with farnesol for 7 days before AAV injection. Black rectangle indicates magnified area (bottom; scale bars, 100 μm). Right: SDH staining intensities are quantified as three different grades (dark, intermediate, or pale) and plotted as a percentile. $n = 3$. (**E**) Immunoblot analysis of PARIS farnesylation, PGC-1α, PARIS, and FTase α expression in TA muscles of 2-month-old PARIS C638S KI mice ± farnesol diet. Farnesol diet was given for 4 weeks. Right: Quantitation of the immunoblots. $n = 3$. (**F**) Immunostaining of MyHC-IIa and laminin in the EDL muscles of C638S KI mice ± farnesol diet. Scale bar, 50 μm. Right: Quantification of MyHC-IIa–positive myofibers, plotted as a percentile. $n = 3$. Data are expressed as mean ± SEM.

showed greatly increased percentages of MyHC-IIa–positive myofibers as compared with mice fed with HFD plus vehicle (Fig. 7E). In addition, the proportion of myofibers with strong SDH activity increased in the GAS muscles of farnesol- or metformin-administrated 6-month-old HFD mice (Fig. 7F). Consistently, farnesol or metformin restored PGC-1α expression in GAS of HFD-fed mice (Fig. 7G). The restoration of PGC-1α expression by farnesol correlated with elevated expression of PARIS farnesylation, whereas metformin led to the down-regulation of total PARIS in HFD-fed mice (Fig. 7G), suggesting that farnesol and metformin exert beneficial effects on HFD-fed mice through different mechanisms.

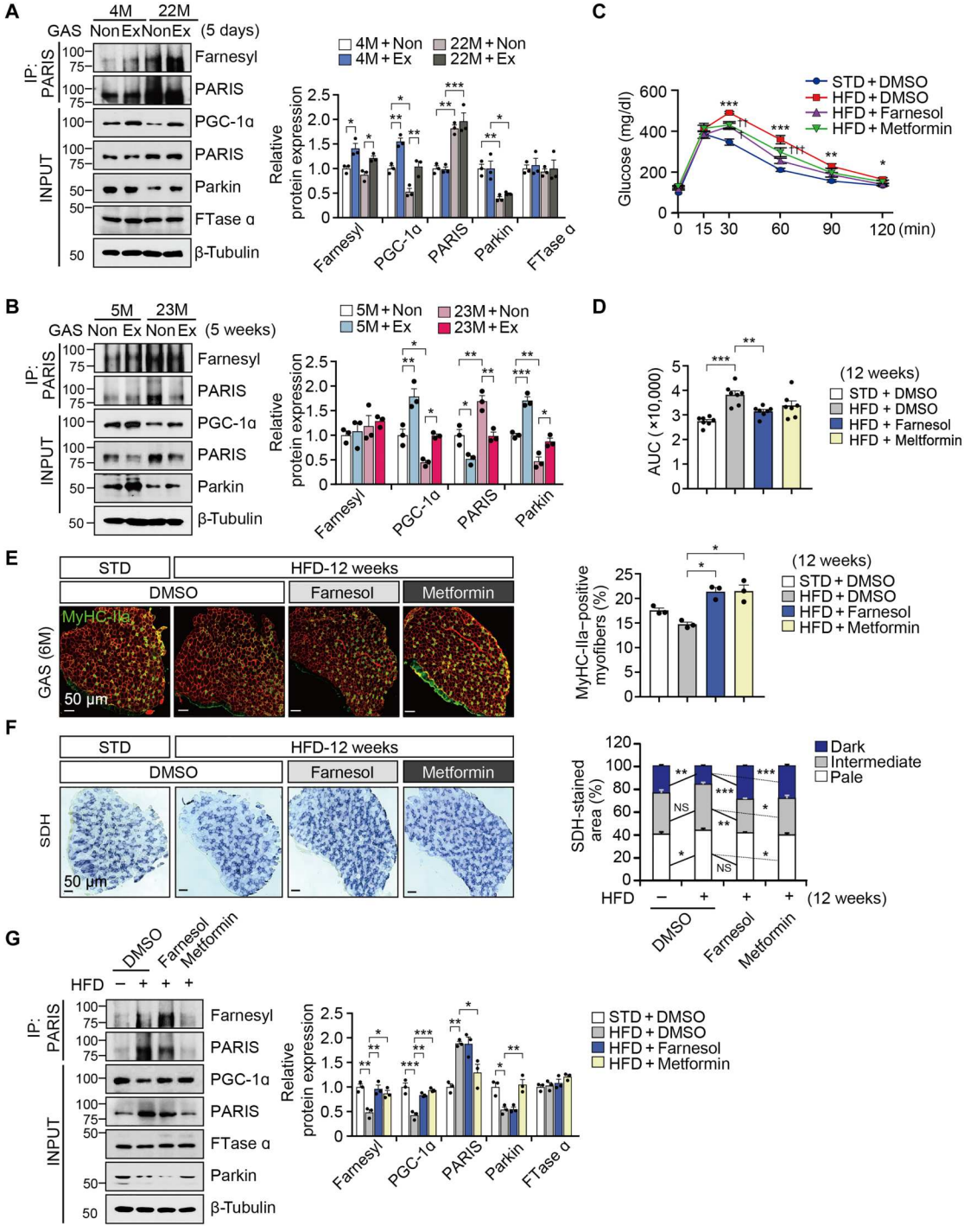

Fig. 7. Farnesol restores PGC-1α in muscles after HFD in mice. (**A**) Immunoblot analysis of PARIS farnesylation in the GAS muscles of 4- and 22-month-old mice after 5 days of exercise (Ex). Non, non-exercised. Right: Quantification. $n = 3$. (**B**) Immunoblot analysis of PARIS farnesylation, PGC-1α, and PARIS expression in the GAS muscles of 5- or 23-month-old mice that were exercised for 5 weeks. Right: Quantification. $n = 3$. (**C**) Glucose tolerance test and (**D**) quantification (AUC) of glucose clearance from mice fed with standard diet (STD), high-fat diet (HFD), HFD + farnesol, or HFD + metformin for 12 weeks. STD, HFD, HFD + farnesol, $n = 8$; HFD + metformin, $n = 7$. (**E**) Immunostaining of MyHC-IIa with the GAS muscles of mice fed with STD, HFD, HFD + farnesol, or HFD + metformin for 12 weeks. Scale bar, 50 μm. Right: Quantification of MyHC-IIa–positive myofibers. $n = 3$. (**F**) Histological staining for SDH activities in the GAS of mice fed with STD, HFD, HFD + farnesol, or HFD + metformin. Scale bar, 50 μm. Right: SDH staining intensities are quantified as three different grades (dark, intermediate, or pale) and plotted as a percentile. $n = 3$. (**G**) Immunoblot analysis of PARIS farnesylation in the GAS muscles of STD, HFD, HFD + farnesol, or HFD + metformin-fed mice. Right: Quantification of farnesylated PARIS, PGC-1α, total PARIS, Parkin, and FTase α. $n = 3$. Data are expressed as mean ± SEM. Statistical significance was determined by two-way ANOVA test (A, B, F, and G) with Tukey post hoc analysis. One-way ANOVA test with Tukey post hoc test was used for (C) ($P < 0.05$; $^{*}P < 0.05$, $^{**}P < 0.01$, and $^{***}P < 0.001$ versus STD; $^{\dagger}P < 0.05$, $^{\dagger\dagger}P < 0.05$, and $^{\dagger\dagger\dagger}P < 0.05$ versus HFD). Differences were considered significant when $P < 0.05$. $^{*}P < 0.05$, $^{**}P < 0.01$, and $^{***}P < 0.001$.

DISCUSSION

In this study, we screened for compounds that induced PGC-1α expression in muscles and identified farnesol as a lead compound. We further demonstrated that farnesol enhanced muscle oxidative metabolism and protected muscles from aging-related muscle weakness and metabolic alterations. The molecular and in vivo functional studies revealed that the effect of farnesol on PGC-1α induction was mediated through the farnesylation of PARIS at the cysteine residue 638.

PPARs (PPARα, PPARγ, and PPARδ) are fundamentally important for energy homeostasis. Among them, PPARα is highly expressed in skeletal muscle and liver and plays a pivotal role in the regulation of lipid homeostasis and fatty acid oxidation (*45*, *46*). Although the exact mechanism was uncharacterized, farnesol was previously introduced to improve metabolic abnormalities in mice via both PPARα-dependent and PPARα-independent pathways (*47*). However, in this study, we found no alteration of PPARα protein and mRNA expression itself or its target genes in C2C12 cells treated with farnesol. These data might suggest that the induction of PPARα by farnesol in vivo can be attributed to indirect stimulation by improvement of whole-body metabolism. Farnesol did not activate PPRE and up-regulate PGC-1α in the absence of PARIS, indicating that PGC-1α induction by farnesol is PPAR independent. Muscle-specific transduction of PPARα in mice induces a fiber-type switch toward more glycolytic fibers accompanied by reduced capacity for endurance exercise. In contrast, mice lacking PPARα show increased numbers of oxidative fibers and improved glucose homeostasis despite the reduction in muscle fatty acid oxidation (*48*, *49*). Thus, the farnesol-mediated improvement of oxidative metabolism in aged or HFD-fed mice might be independent of PPARα. Moreover, the expression of PPARα protein was not altered in the muscles after knockdown of PARIS (fig. S9G). These data suggest that the farnesol effect and PARIS do not directly involve PPARα.

Because of the well-known preventive effect of exercise on muscle weakness and sarcopenia, the identification of exercise mimetics that can be used safely in aging populations has been actively pursued. Several exercise mimetics activating the upstream of PGC-1α, such as AICAR and GW1516, have shown the potential for clinical use to treat sarcopenia or conditions related to physical immobility (*24*). However, these compounds have potential side effects, such as increased risks of heart defects and cancers (*50*, *51*). Encouragingly, there was no cardiac hypertrophy observed in farnesol-treated mice (fig. S2G). Consistent with the positive effect of PGC-1α on prevention of muscle weakness and aging, farnesol treatment in young and aged mice enhanced oxidative muscle metabolism and muscle strength. In addition, farnesol improved whole-body metabolism in aged mice or HFD-fed mice, which was accompanied by enhanced energy expenditure. Farnesol treatment appears to be more effective in improving muscle strength than muscle mass in aged mice. In humans, the loss of muscle strength occurs faster than that of muscle mass during aging (*1*, *2*), and impaired muscle strength seems to be more closely associated with mortality during aging (*52*). Similar to the effect of AICAR on muscle strength in sedentary mice, farnesol improved muscle function and metabolism in sedentary mice. As with other exercise mimetics, the combination of farnesol treatment and exercise may be an effective strategy to boost its beneficial effect.

Aging-related muscle loss increases susceptibility to falls and physical injury requiring tissue stem cell function including muscle stem cells (*15*, *16*). In aging, muscle satellite cell number and regenerative capacity decline, contributing to impaired muscle regeneration and muscle wasting (*16*). Thus, enhancing muscle satellite cell function is important for muscle maintenance. Our current data suggest that the beneficial effect of farnesol on muscle might be partly due to enhanced satellite cell function and maintenance. Our findings are in agreement with recent publications reporting the important role of PGC-1α in muscle stem cell function and regeneration through modulation of inflammatory response, suppression of fibrosis, and niche remodeling (*19*, *20*, *36*). Because farnesol can induce PGC-1α in muscle as well as muscle stem cells, similar mechanisms might function to improve directly and indirectly muscle stem cell function through niche remodeling and inflammatory response modulation. In addition, the effect of farnesol in muscle stem cell function can be mediated directly via PARIS inhibition. Our previous study has shown that PARIS overexpression in myoblasts triggered oxidative stress–related FoxO1 and p53 activation, leading to cellular senescence and reduced proliferation (*32*). Therefore, further studies are required to elucidate the exact role of PARIS in muscle satellite cell function and maintenance during aging.

This study suggests that Parkin is decreased in aged muscle, leading to PARIS up-regulation. A similar mechanism has been reported in neurodegeneration related to PD (*28*), implying a common mechanism underlying PARIS regulation. Farnesol restores PGC-1α expression in skeletal muscles, suggesting that the farnesylation of PARIS represents a more general mechanism for inhibiting PARIS action on PGC-1α repression in muscles. Considering the metabolic restoration on aged muscles by farnesol, PARIS inhibition might be important for preventing muscle aging and degeneration. The beneficial effect of farnesol on systemic metabolism is not likely to occur entirely through PARIS farnesylation, and there are likely to be other targets of PARIS, contributing to oxidative fiber–specific gene expression in the presence of farnesol. PARIS seems to be inhibited via farnesylation or down-regulation by exercise, farnesol, or metformin in muscles, contributing to PGC-1α induction. Our previous study observed a similar phenomenon in the brains of mice fed with HFD, and metformin enhanced the solubility of Parkin, modulating the PARIS–PGC-1α pathway (*53*). PARIS farnesylation affects its ability to bind chromatin, rather than its cellular localization, as observed in myoblasts or in brain (*54*). Further study will be required to define the distinct regulatory mechanisms of PARIS accumulation in aged muscles. Together, our study suggests that farnesol and other compounds that target the PARIS–PGC-1α pathway could be further evaluated as a potential treatment for aging-associated muscle weakness.

MATERIALS AND METHODS

Study design

The objectives of this study are (i) to identify a PGC-1α inducer, a key factor exerting the beneficial effects of exercise in skeletal muscle, and (ii) to analyze its protective effects and underlying molecular mechanisms on muscle weakness related to aging or pathological conditions. We performed HTS of about 2552 compounds in C2C12 myoblasts expressing PGC-1α reporters and selected farnesol. To analyze the effect of farnesol, we used multiple experimental

models, and the number of mice used in this study is presented in table S2. To evaluate the effect of farnesol in muscle weakness related to aging or obesity, we used young mice (4 to 7 months old), aged mice (23 to 26 months old), or age-matched normal or HFD-induced obesity mice. The farnesol-mediated effects on muscle aging and metabolic characteristics were assessed by analyzing muscle strength, metabolic parameters, and muscle fiber phenotypes by histochemistry, immunostaining, and RNA sequencing. To analyze the effect of farnesol in muscle regeneration capacity, we used young (3 months old) and aged (26 months old) mice for CTX injection and farnesol treatment. In addition, muscles of young mice were transduced with control or PARIS-expressing lentivirus or AAV virus to analyze the role of PARIS in farnesol-mediated effects. To understand molecular mechanisms underlying farnesol effects mediated through PARIS, we used DMSO or farnesol-treated C2C12 myoblasts expressing PARIS WT or C631S mutant as well as age-matched PARIS WT or C631S mutant mice. To examine the exercise effect on PARIS-mediated PGC-1α regulation, mice were subjected to short-term (5 days) and long-term (5 weeks) treadmill exercise, and muscles were analyzed for PARIS abundance and farnesylation. Detailed information for replicates and statistical analysis is described in figure legends and data file S1. Animal experiments were carried out in a blinded manner. Animal experiments were conducted by the Public Health Service Policy on Humane Care and Use of Laboratory Animals and were approved by the Institutional Animal Care and Research Advisory Committee at Sungkyunkwan University School of Medicine Laboratory Animal Research Center and laboratory animal resource center of Daegu Gyeongbuk Institute of Science and Technology (DGIST). Detailed methods and materials are described in the Supplementary Materials.

Statistical analysis

Data are expressed as mean ± SEM or mean ± SD. Statistical significance was determined by applying unpaired Student's *t* test or analysis of variance (ANOVA) test (one or two) with Tukey post hoc analysis. Differences were considered significant when $P < 0.05$. $^{*}P < 0.05$, $^{**}P < 0.01$, and $^{***}P < 0.001$. Details regarding numbers of replicates, the definition of center/error bars, and statistical methods can be found in the figure legends. Exact *P* values and which statistical methods were used can be found in data file S1.

Supplementary Materials

This PDF file includes:
Materials and Methods
Figs. S1 to S12
Table S1 to S4
References (*55*, *56*)

Other Supplementary Material for this manuscript includes the following:
Data file S1
MDAR Reproducibility Checklist

REFERENCES AND NOTES

1. B. H. Goodpaster, S. W. Park, T. B. Harris, S. B. Kritchevsky, M. Nevitt, A. V. Schwartz, E. M. Simonsick, F. A. Tylavsky, M. Visser, A. B. Newman, The loss of skeletal muscle strength, mass, and quality in older adults: The health, aging and body composition study. *J. Gerontol. A Biol. Sci. Med. Sci.* **61**, 1059–1064 (2006).
2. E. J. Metter, N. Lynch, R. Conwit, R. Lindle, J. Tobin, B. Hurley, Muscle quality and age: Cross-sectional and longitudinal comparisons. *J. Gerontol. A. Biol. Sci. Med. Sci.* **54**, B207–B218 (1999).
3. K. S. Nair, Aging muscle. *Am. J. Clin. Nutr.* **81**, 953–963 (2005).
4. S. Stenholm, T. B. Harris, T. Rantanen, M. Visser, S. B. Kritchevsky, L. Ferrucci, Sarcopenic obesity: Definition, cause and consequences. *Curr. Opin. Clin. Nutr. Metab. Care* **11**, 693–700 (2008).
5. E. Volpi, R. Nazemi, S. Fujita, Muscle tissue changes with aging. *Curr. Opin. Clin. Nutr. Metab. Care* **7**, 405–410 (2004).
6. R. R. Wolfe, The underappreciated role of muscle in health and disease. *Am. J. Clin. Nutr.* **84**, 475–482 (2006).
7. B. Egan, J. R. Zierath, Exercise metabolism and the molecular regulation of skeletal muscle adaptation. *Cell Metab.* **17**, 162–184 (2013).
8. J. Holloszy, Regulation by exercise of skeletal muscle content of mitochondria and GLUT4. *J. Physiol. Pharmacol.* **59** (Suppl 7), 5–18 (2008).
9. J. F. Gill, G. Santos, S. Schnyder, C. Handschin, PGC-1α affects aging-related changes in muscle and motor function by modulating specific exercise-mediated changes in old mice. *Aging Cell* **17**, e12697 (2018).
10. S. V. Yang, E. Loro, S. Wada, B. Kim, W. J. Tseng, K. T. Li, T. S. Khurana, Z. Arany, Functional effects of muscle PGC-1alpha in aged animals. *Skelet. Muscle* **10**, 14 (2020).
11. Z. Arany, S.-Y. Foo, Y. Ma, J. L. Ruas, A. Bommi-Reddy, G. Girnun, M. Cooper, D. Laznik, J. Chinsomboon, S. M. Rangwala, K. H. Baek, A. Rosenzweig, B. M. Spiegelman, HIF-independent regulation of VEGF and angiogenesis by the transcriptional coactivator PGC-1α. *Nature* **451**, 1008–1012 (2008).
12. J. Lin, H. Wu, P. T. Tarr, C.-Y. Zhang, Z. Wu, O. Boss, L. F. Michael, P. Puigserver, E. Isotani, E. N. Olson, B. B. Lowell, R. Bassel-Duby, B. M. Spiegelman, Transcriptional co-activator PGC-1α drives the formation of slow-twitch muscle fibres. *Nature* **418**, 797–801 (2002).
13. T. C. Leone, J. J. Lehman, B. N. Finck, P. J. Schaeffer, A. R. Wende, S. Boudina, M. Courtois, D. F. Wozniak, N. Sambandam, C. Bernal-Mizrachi, Z. Chen, J. O. Holloszy, D. M. Medeiros, R. E. Schmidt, J. E. Saffitz, E. D. Abel, C. F. Semenkovich, D. P. Kelly, PGC-1α deficiency causes multi-system energy metabolic derangements: Muscle dysfunction, abnormal weight control and hepatic steatosis. *PLOS Biol.* **3**, e101 (2005).
14. M. Sandri, J. Lin, C. Handschin, W. Yang, Z. P. Arany, S. H. Lecker, A. L. Goldberg, B. M. Spiegelman, PGC-1alpha protects skeletal muscle from atrophy by suppressing FoxO3 action and atrophy-specific gene transcription. *Proc. Natl. Acad. Sci. U.S.A.* **103**, 16260–16265 (2006).
15. S.-K. Lim, J. Beom, S. Y. Lee, B. R. Kim, S.-W. Chun, J.-Y. Lim, E. Shin Lee, Association between sarcopenia and fall characteristics in older adults with fragility hip fracture. *Injury* **51**, 2640–2647 (2020).
16. S. E. Alway, M. J. Myers, J. S. Mohamed, Regulation of satellite cell function in sarcopenia. *Front. Aging Neurosci.* **6**, 246 (2014).
17. C. J. Mann, E. Perdiguero, Y. Kharraz, S. Aguilar, P. Pessina, A. L. Serrano, P. Muñoz-Cánoves, Aberrant repair and fibrosis development in skeletal muscle. *Skelet. Muscle* **1**, 21 (2011).
18. L.-E. Thornell, Sarcopenic obesity: Satellite cells in the aging muscle. *Curr. Opin. Clin. Nutr. Metab. Care* **14**, 22–27 (2011).
19. I. Dinulovic, R. Furrer, M. Beer, A. Ferry, B. Cardel, C. Handschin, Muscle PGC-1α modulates satellite cell number and proliferation by remodeling the stem cell niche. *Skelet. Muscle* **6**, 39 (2016).
20. I. Dinulovic, R. Furrer, S. Di Fulvio, A. Ferry, M. Beer, C. Handschin, PGC-1α modulates necrosis, inflammatory response, and fibrotic tissue formation in injured skeletal muscle. *Skelet. Muscle* **6**, 38 (2016).
21. M. Beltrà, F. Pin, D. Costamagna, R. Duelen, A. Renzini, R. Ballarò, L. Garcia-Castillo, A. Iannuzzi, V. Moresi, D. Coletti, M. Sampaolesi, F. Penna, P. Costelli, PGC-1α in the myofibers regulates the balance between myogenic and adipogenic progenitors affecting muscle regeneration. *iScience* **25**, 105480 (2022).
22. A.-S. Arnold, A. Egger, C. Handschin, PGC-1α and myokines in the aging muscle—A mini-review. *Gerontology* **57**, 37–43 (2011).
23. X. Wan, X. Zhu, H. Wang, Y. Feng, W. Zhou, P. Liu, W. Shen, L. Zhang, L. Liu, T. Li, D. Diao, F. Yang, Q. Zhao, L. Chen, J. Ren, S. Yan, J. Li, C. Yu, Z. Ju, PGC1α protects against hepatic steatosis and insulin resistance via enhancing IL10-mediated anti-inflammatory response. *FASEB J.* **34**, 10751–10761 (2020).
24. W. G. Aschenbach, M. F. Hirshman, N. Fujii, K. Sakamoto, K. F. Howlett, L. J. Goodyear, Effect of AICAR treatment on glycogen metabolism in skeletal muscle. *Diabetes* **51**, 567–573 (2002).
25. V. A. Narkar, M. Downes, R. T. Yu, E. Embler, Y.-X. Wang, E. Banayo, M. M. Mihaylova, M. C. Nelson, Y. Zou, H. Juguilon, H. Kang, R. J. Shaw, R. M. Evans, AMPK and PPARδ agonists are exercise mimetics. *Cell* **134**, 405–415 (2008).
26. K. Svensson, C. Handschin, Modulation of PGC-1α activity as a treatment for metabolic and muscle-related diseases. *Drug Discov. Today* **19**, 1024–1029 (2014).

27. W. Fan, R. M. Evans, Exercise mimetics: Impact on health and performance. *Cell Metab.* **25**, 242–247 (2017).
28. J.-H. Shin, H. S. Ko, H. Kang, Y. Lee, Y.-I. Lee, O. Pletinkova, J. C. Troconso, V. L. Dawson, T. M. Dawson, PARIS (ZNF746) repression of PGC-1α contributes to neurodegeneration in Parkinson's disease. *Cell* **144**, 689–702 (2011).
29. D. A. Stevens, Y. Lee, H. C. Kang, B. D. Lee, Y.-I. Lee, A. Bower, H. Jiang, S.-U. Kang, S. A. Andrabi, V. L. Dawson, J.-H. Shin, T. M. Dawson, Parkin loss leads to PARIS-dependent declines in mitochondrial mass and respiration. *Proc. Natl. Acad. Sci. U.S.A.* **112**, 11696–11701 (2015).
30. I. E. Clark, M. W. Dodson, C. Jiang, J. H. Cao, J. R. Huh, J. H. Seol, S. J. Yoo, B. A. Hay, M. Guo, Drosophila pink1 is required for mitochondrial function and interacts genetically with parkin. *Nature* **441**, 1162–1166 (2006).
31. H. Mortiboys, K. J. Thomas, W. J. Koopman, S. Klaffke, P. Abou-Sleiman, S. Olpin, N. W. Wood, P. H. Willems, J. A. Smeitink, M. R. Cookson, O. Bandmann, Mitochondrial function and morphology are impaired in parkin-mutant fibroblasts. *Ann. Neurol.* **64**, 555–565 (2008).
32. J.-H. Bae, H.-J. Jeong, H. Kim, Y.-E. Leem, D. Ryu, S. C. Park, Y.-I. Lee, S. C. Cho, J.-S. Kang, ZNF746/PARIS overexpression induces cellular senescence through FoxO1/p21 axis activation in myoblasts. *Cell Death Dis.* **11**, 359 (2020).
33. P. A. Edwards, J. Ericsson, Sterols and isoprenoids: Signaling molecules derived from the cholesterol biosynthetic pathway. *Annu. Rev. Biochem.* **68**, 157–185 (1999).
34. J. L. Ruas, J. P. White, R. R. Rao, S. Kleiner, K. T. Brannan, B. C. Harrison, N. P. Greene, J. Wu, J. L. Estall, B. A. Irving, I. R. Lanza, K. A. Rasbach, M. Okutsu, K. S. Nair, Z. Yan, L. A. Leinwand, B. M. Spiegelman, A PGC-1α isoform induced by resistance training regulates skeletal muscle hypertrophy. *Cell* **151**, 1319–1331 (2012).
35. J. Chinsomboon, J. Ruas, R. K. Gupta, R. Thom, J. Shoag, G. C. Rowe, N. Sawada, S. Raghuram, Z. Arany, The transcriptional coactivator PGC-1alpha mediates exercise-induced angiogenesis in skeletal muscle. *Proc. Natl. Acad. Sci. U.S.A.* **106**, 21401–21406 (2009).
36. D. Haralampieva, S. Salemi, T. Betzel, I. Dinulovic, S. D. Kramer, R. Schibli, T. Sulser, C. Handschin, S. M. Ametamey, D. Eberli, Injected human muscle precursor cells overexpressing PGC-1α enhance functional muscle regeneration after trauma. *Stem Cells Int.* **2018**, 1–11 (2018).
37. P. M. Coen, R. V. Musci, J. M. Hinkley, B. F. Miller, Mitochondria as a target for mitigating sarcopenia. *Front. Physiol.* **9**, 1883 (2019).
38. E. Migliavacca, S. K. H. Tay, H. P. Patel, T. Sonntag, G. Civiletto, C. McFarlane, T. Forrester, S. J. Barton, M. K. Leow, E. Antoun, A. Charpagne, Y. S. Chong, P. Descombes, L. Feng, P. Francis-Emmanuel, E. S. Garratt, M. P. Giner, C. O. Green, S. Karaz, N. Kothandaraman, J. Marquis, S. Metairon, S. Moco, G. Nelson, S. Ngo, T. Pleasants, F. Raymond, A. A. Sayer, C. M. Sim, J. Slater-Jefferies, H. E. Syddall, P. F. Tan, P. Titcombe, C. Vaz, L. D. Westbury, G. Wong, Y. H. Wu, C. Cooper, A. Sheppard, K. M. Godfrey, K. A. Lillycrop, N. Karnani, J. N. Feige, Mitochondrial oxidative capacity and NAD^+ biosynthesis are reduced in human sarcopenia across ethnicities. *Nat. Commun.* **10**, 5808 (2019).
39. D. J. Ham, A. Börsch, S. Lin, M. Thürkauf, M. Weihrauch, J. R. Reinhard, J. Delezie, F. Battilana, X. Wang, M. S. Kaiser, M. Guridi, M. Sinnreich, M. M. Rich, N. Mittal, L. A. Tintignac, C. Handschin, M. Zavolan, M. A. Ruegg, The neuromuscular junction is a focal point of mTORC1 signaling in sarcopenia. *Nat. Commun.* **11**, 4510 (2020).
40. S. Jäger, C. Handschin, J. St-Pierre, B. M. Spiegelman, AMP-activated protein kinase (AMPK) action in skeletal muscle via direct phosphorylation of PGC-1α. *Proc. Natl. Acad. Sci. U.S.A.* **104**, 12017–12022 (2007).
41. R. W. J. Hangelbroek, P. Fazelzadeh, M. Tieland, M. V. Boekschoten, G. J. E. J. Hooiveld, J. P. M. van Duynhoven, J. A. Timmons, L. B. Verdijk, L. C. P. G. M. de Groot, L. J. C. van Loon, M. Müller, Expression of protocadherin gamma in skeletal muscle tissue is associated with age and muscle weakness. *J. Cachexia Sarcopenia Muscle* **7**, 604–614 (2016).
42. N. Takahashi, T. Kawada, T. Goto, T. Yamamoto, A. Taimatsu, N. Matsui, K. Kimura, M. Saito, M. Hosokawa, K. Miyashita, T. Fushiki, Dual action of isoprenols from herbal medicines on both PPARgamma and PPARalpha in 3T3-L1 adipocytes and HepG2 hepatocytes. *FEBS Lett.* **514**, 315–322 (2002).
43. H. C. Hang, M. E. Linder, Exploring protein lipidation with chemical biology. *Chem. Rev.* **111**, 6341–6358 (2011).
44. L. M. Sparks, H. Xie, R. A. Koza, R. Mynatt, M. W. Hulver, G. A. Bray, S. R. Smith, A high-fat diet coordinately downregulates genes required for mitochondrial oxidative phosphorylation in skeletal muscle. *Diabetes* **54**, 1926–1933 (2005).
45. O. Braissant, F. Foufelle, C. Scotto, M. Dauça, W. Wahli, Differential expression of peroxisome proliferator-activated receptors (PPARs): Tissue distribution of PPAR-alpha, -beta, and -gamma in the adult rat. *Endocrinology* **137**, 354–366 (1996).
46. K. S. Frederiksen, E. M. Wulff, P. Sauerberg, J. P. Mogensen, L. Jeppesen, J. Fleckner, Prediction of PPAR-α ligand-mediated physiological changes using gene expression profiles. *J. Lipid Res.* **45**, 592–601 (2004).
47. T. Goto, Y.-I. Kim, K. Funakoshi, A. Teraminami, T. Uemura, S. Hirai, J.-Y. Lee, M. Makishima, R. Nakata, H. Inoue, H. Senju, M. Matsunaga, F. Horio, N. Takahashi, T. Kawada, Farnesol, an isoprenoid, improves metabolic abnormalities in mice via both PPARα-dependent and -independent pathways. *Am. J. Physiol. Endocrinol. Metab.* **301**, E1022–E1032 (2011).
48. B. N. Finck, C. Bernal-Mizrachi, D. H. Han, T. Coleman, N. Sambandam, L. L. LaRiviere, J. O. Holloszy, C. F. Semenkovich, D. P. Kelly, A potential link between muscle peroxisome proliferator-activated receptor-α signaling and obesity-related diabetes. *Cell Metab.* **1**, 133–144 (2005).
49. Z. Gan, J. Rumsey, B. C. Hazen, L. Lai, T. C. Leone, R. B. Vega, H. Xie, K. E. Conley, J. Auwerx, S. R. Smith, E. N. Olson, A. Kralli, D. P. Kelly, Nuclear receptor/microRNA circuitry links muscle fiber type to energy metabolism. *J. Clin. Invest.* **123**, 2564–2575 (2013).
50. S. Han, J. D. Ritzenthaler, X. Sun, Y. Zheng, J. Roman, Activation of peroxisome proliferator–activated receptor β/δ induces lung cancer growth via peroxisome proliferator–activated receptor coactivator γ-1α. *Am. J. Respir. Cell Mol. Biol.* **40**, 325–331 (2009).
51. A. Sahebkar, G. T. Chew, G. F. Watts, New peroxisome proliferator-activated receptor agonists: Potential treatments for atherogenic dyslipidemia and non-alcoholic fatty liver disease. *Expert Opin. Pharmacother.* **15**, 493–503 (2014).
52. E. J. Metter, L. A. Talbot, M. Schrager, R. Conwit, Skeletal muscle strength as a predictor of all-cause mortality in healthy men. *J. Gerontol. A Biol. Sci. Med. Sci.* **57**, B359–B365 (2002).
53. R. Khang, C. Park, J. H. Shin, Dysregulation of parkin in the substantia nigra of db/db and high-fat diet mice. *Neuroscience* **294**, 182–192 (2015).
54. A. Jo, Y. Lee, T.-I. Kam, S.-U. Kang, S. Neifert, S. S. Karuppagounder, R. Khang, H. Kang, H. Park, S.-C. Chou, S. Oh, H. Jiang, D. A. Swing, S. Ham, S. Pirooznia, G. K. E. Umanah, X. Mao, M. Kumar, H. S. Ko, H. C. Kang, B. D. Lee, Y.-I. Lee, S. A. Andrabi, C.-H. Park, J.-Y. Lee, H. Kim, H. Kim, H. Kim, J. W. Cho, S. H. Paek, C. H. Na, L. Tessarollo, V. L. Dawson, T. M. Dawson, J.-H. Shin, PARIS farnesylation prevents neurodegeneration in models of Parkinson's disease. *Sci. Transl. Med.* **13**, eaax8891 (2021).
55. K. Teshima, T. Kondo, Analytical method for determination of allylic isoprenols in rat tissues by liquid chromatography/tandem mass spectrometry following chemical derivatization with 3-nitrophtalic anhydride. *J. Pharm. Biomed. Anal.* **47**, 560–566 (2008).
56. L. Henneman, A. G. van Cruchten, S. W. Denis, M. W. Amolins, A. T. Placzek, R. A. Gibbs, W. Kulik, H. R. Waterham, Detection of nonsterol isoprenoids by HPLC–MS/MS. *Anal. Biochem.* **383**, 18–24 (2008).

Acknowledgments

Funding: This research was supported by the Well Aging Research Center at the Samsung Advanced Institute of Technology. This research was also supported by grants from the NRF (NRF-2022R1A2B5B02001482 and 2016R1A5A2945889 to J.-S.K.; 2017R1E1A1A01073945, 2016R1A5A2945889, and 2023R1A2C1003347 to J.-H.S.; 2020M3A9D8038653 and 2021R1A2C1009107 to Y.-I.L.; and 2020R1A2C2009439 to S.C.P.) funded by the Korea Ministry of Science, ICT and Future Planning (MSIP) and by a Korea Basic Science Institute (National Research Facilities and Equipment Center) grant funded by the Ministry of Education (2020R1A6C101A191 to J.-H.S.). The chemical library used in this study was provided by Korea Chemical Bank of Korea Research Institute of Chemical Technology (http://chembank.org/). This work was supported by grants from the JPB Foundation, the Cure Parkinson's Trust, and the Bachmann-Strauss Dystonia and Parkinson Foundation to T.M.D. We acknowledge the joint participation by the Adrienne Helis Malvin Medical Research Foundation and the Diana Helis Henry Medical Research Foundation through its direct engagement in the continuous active conduct of medical research in conjunction with the Johns Hopkins Hospital and the Johns Hopkins University School of Medicine and the Foundation's Parkinson's Disease Programs M-1, M-2, and H-2014 to T.M.D. and V.L.D. T.M.D. is the Leonard and Madlyn Abramson Professor in Neurodegenerative Diseases. **Author contributions:** J.-S.K., J.-H.S., T.M.D., and S.C.P. supervised the project. J.-S.K., J.-H.S., S.C.P., and S.C.C. formulated the hypothesis. J.-H.S., R.K., and A.J. designed and performed high-throughput chemical screening. J.-S.K., J.-H.S., S.C.P., Y.-I.L., S.C.C., T.-I.K., C.-L.Y., and E.S.S. designed in vivo experiments. E.S.S., J.-H.B., H.-J.J., M.-H.J., Y.-I.L., T.-I.K., and S.C.C. performed mice functional analysis. J.-H.B. and H.-J.J. performed immunocytochemistry. J.-H.B., A.J., H. Kim, M.-H.J., S.C.C., and H. Kang performed immunoblotting and qRT-PCR and analyzed the results. Y.W.H. performed mass spectrometric analysis. J.-H.B., S.O.S., S.C.C., M.S.K., and Y.J. performed RNA-sequencing analysis and data analysis. A.J., H.-J.J., and S.C.C. performed the intramuscular virus injections. T.M.D., V.L.D., and Y.-I.L. provided critical suggestions in interpreting and analyzing data. J.-S.K., J.-H.S., S.C.P., S.C.C., J.-H.B., J.P., T.-I.K., and A.J. initiated and organized the study and wrote the manuscript. All authors contributed to writing the final manuscript. **Competing interests:** J.-H.B., A.J., S.C.C., H.-J.J., E.S.S., S.C.P., J.-H.S., and J.-S.K. have filed patents entitled "Composition comprising farnesol and use thereof" (US20160089340A1). J.-S.K. is a founder of AniMusCure Inc. and holds an ownership equity interest in the company. These arrangements have been reviewed and approved by the Sungkyunkwan University in accordance with its conflict of interest policies. T.M.D. is a member of the Linked Clinical Trials Committee. T.M.D. and V.L.D. are founders of Valted LLC and hold an ownership equity interest in the company. These arrangements have been reviewed and approved by the Johns Hopkins University in accordance with its conflict of interest policies. Patents related to this work include US9274128B2 entitled "Transcriptional repression leading to Parkinson's disease" and WO2017161155A1 "Methods for preventing or treating Parkinson's disease by the farnesylation of PARIS." The other authors declare that they

have no competing interests. **Data and materials availability:** All data associated with this study are present in the paper or the Supplementary Materials. RNA-sequencing data have been deposited in GEO database under accession code GSE240281.

Submitted 3 March 2021
Resubmitted 27 February 2023
Accepted 11 August 2023
Published 30 August 2023
10.1126/scitranslmed.abh3489

Science Translational Medicine

Farnesol prevents aging-related muscle weakness in mice through enhanced farnesylation of Parkin-interacting substrate

Ju-Hyeon Bae, Areum Jo, Sung Chun Cho, Yun-Il Lee, Tae-In Kam, Chang-Lim You, Hyeon-Ju Jeong, Hyebeen Kim, Myong-Ho Jeong, Yideul Jeong, Young Wan Ha, Yu Seon Kim, Jiwoon Kim, Seung-Hwa Woo, Minseok S. Kim, Eui Seok Shin, Sang Ok Song, Hojin Kang, Rin Khang, Soojeong Park, Joobae Park, Valina L. Dawson, Ted M. Dawson, Sang Chul Park, Joo-Ho Shin, and Jong-Sun Kang

Sci. Transl. Med., **15** (711), eabh3489.
DOI: 10.1126/scitranslmed.abh3489

Science Translational Medicine (ISSN) is published by the American Association for the Advancement of Science. 1200 New York Avenue NW, Washington, DC 20005. The title *Science Translational Medicine* is a registered trademark of AAAS.